Dynamic response optimization

of an

acoustic guitar

Martijn van Boven

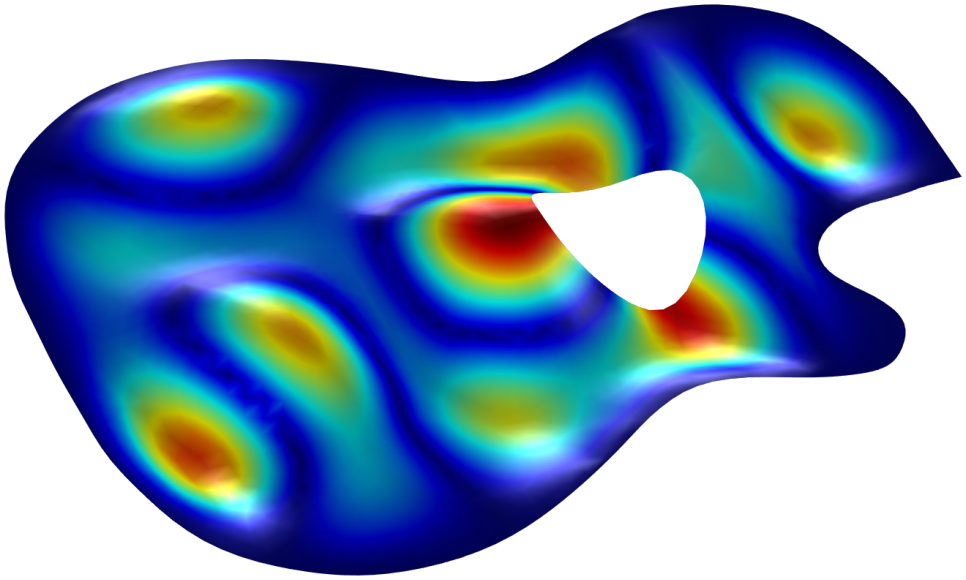

TU Delft Delft University of Technology

Dynamic response optimization

of an

acoustic guitar

Master Thesis

M.M.A. van Boven

in partial fulfilment of the requirements for the degree of

Master of Science

in Mechanical Engineering

at Delft University of Technology

Department:	Precision and Microsystems Engineering
Research group:	Structural Optimization and Mechanics
Coach:	dr.ir. M. Langelaar
Professor:	prof.dr.ir. A. van Keulen
Student number:	4012356
Graduation date:	17th January 2017
Report no:	EM 2017.010
Contact:	info@martijnvanboven.com

TU Delft Delft University of Technology

Summary

Currently the production process of acoustic guitar factories does not result in instruments with equal dynamical behaviour, due to the varying material properties of wood from tree to tree. Experienced individual guitar builders are able to handle those material variations, but this is a labour intensive process because there is no structured methodology available about how to obtain a certain desired frequency response.

In this study it is investigated if the perceived sound produced by a guitar is controllable by using dynamic response optimization methods in order to adjust geometric design parameters during the production process. The goal is to find a method which is both able to improve the consistency between mass-produced instruments and to decrease the required building time of handbuilt guitars. Until now no research is available which uses optimization methods in order to shape the dynamic response of a guitar over a range of frequencies.

Previous research presented an analytical model which is able to give a quantitative description of a guitar's dynamic response. The response is characterized by a measurement of the sound pressure level at 1 meter distance over a range of excitation frequencies. It was shown that the sound of a guitar is mainly determined by the dynamic behaviour of its top plate. This study uses a finite element model in order to estimate the effect of geometric design variations. The finite element model is used in combination with an optimization algorithm which shapes the dynamic response to a certain desired response. Due to this optimization approach the finite element model needs to be evaluated for many combinations of design variables. A computationally cheap finite element model is needed to approximate the physical behaviour of the guitar its top plate.

Based on the results of the optimization algorithm it is concluded that it is indeed possible to control the perceived sound produced by a guitar, by using dynamic response optimization methods in order to adjust geometric design parameters during the production process. Although some aspects need to be worked out further before the approach presented in this research can be implemented in a production process, the theoretical background will definitely be useful in order to improve consistency between instruments by using frequency response measurements during the building process.

Table of Contents

1 Introduction

Acoustic guitars have been used for a few centuries in order to make music, either as a solo instrument or in combination with other instruments or vocalists. Many different types of guitars are available, enabling the player to choose a guitar which produces a sound that suits his or her needs.
Figure 1 and 2 depicture the interior of a guitar its soundbox. The guitar shown was built in 2013 by the author of this report. The soundbox consists of a top and back plate which are connected by the sides. Stiffeners, named braces, are attached to both the top and back plate. The sound of a guitar is mainly determined by the dynamic response of this construction, which makes it very interesting from an engineering point of view [13].

Figure 1: Guitar interior.

Figure 2: Close-up of the braces attached to the top plate.

The production process of acoustic guitars can roughly be subdivided into two branches. Most guitars are built in mass production environments in big factories. Apart from this a small part of the guitars sold are hand-built by individual guitar builders, named luthiers, who generally produce the more expensive and desirable instruments. Both ways of guitar building bring some difficulties which will be explained now.

Guitar manufacturers and many luthiers use fixed dimensions for every guitar of a particular model. But if we zoom in on the palette of sounds created by different guitars, the sound produced by a guitar is also influenced by material property variations and sometimes production inaccuracies [1]. Due to the varying density, stiffness and damping properties of wood from tree to tree this building approach does not result in instruments with equal dynamical behaviour. A better approach would be to aim for a certain frequency response of the guitar as this leads to less differences between instruments which are supposed to sound the same.

The most reputable luthiers are usually already looking for a certain frequency response of the surface areas while building their instrument. This approach is called "voicing" the guitar, which involves knocking on the wood, chiseling, scraping and sanding the material until they consider the "tap tone" to be right [3]. As currently no structured methodology is available about how to voice a guitar this is somewhat like reinventing the wheel over and over again for every build, causing it to be a labour intensive process which can take days or even weeks.

Many literature is available about acoustic guitar design and building [1][2][3]. Understanding the dynamic behaviour of a guitar, either obtained by decades of building experience or by studying the theoretical aspects of structural dynamics, is a valuable skill which will definitely help one to produce a more desirable instrument. Although one should never underestimate the skills of experienced craftsmen, occasionally statements about the effects of geometrical design choices are encountered which are highly questionable from a theoretical point of view. Also there still is a lot unknown about the effect of some design choices on the sound of the finished instrument.

Although guitars have been made out of wood for centuries, apart from the material property variations wood is also not an ideal material due to its hygroscopic properties [23]. Moreover, high quality woods are getting scarce due to regulations and deforestation [24]. A better understanding of shaping the frequency response of a guitar might open up possibilities for the use of synthetic materials.

Research question

Based on the above-mentioned considerations the research question is formulated as follows: *Is the perceived sound produced by a guitar controllable by using dynamic response optimization methods in order to adjust geometric design parameters during the production process?*

In order to answer this question, first it is investigated whether the properties which characterize a certain guitar can be captured and approximated by an analytical model. Subsequently such a model could be used in combination with a finite element model and an optimization algorithm during a guitar's production process to remove inconsistencies in the dynamic response caused by material property variations.
If the answer to the research question is positive, it should be possible to improve consistency between mass-produced instruments by using frequency response measurements during the building process. Apart from this it will also enable traditional luthiers to shorten the voicing process, as this scientific approach could give them a structured way of shaping the frequency response of the soundbox.

Scope of the research

This thesis is not about how to design a guitar which sounds "good" or "better". It is an exploratory research about finding a methodology which might be used in practice to decrease the required building time of a guitar without sacrificing quality, meanwhile improving consistency between instruments. Until now no research is available which uses an optimization approach in order to shape the dynamic response of a guitar over a range of frequencies. Almost no attention will be paid to the psychoacoustics part of music. Instead, the research is aimed at finding an objective way of representing the important aspects which characterize a certain sound.

The approach presented in this paper is not only applicable to guitar building but to a broad range of acoustic, preferably stringed, instruments. Possibly parts of this research may also be relevant in completely different areas. Theory about shaping the sound produced by vibrating surfaces could also be of interest in the field of noise reduction of structures, for example wind turbines.

Structure of the report

Part 1 of this report presents a literature study, which shows that in the past 40 years many research papers on acoustic guitar modelling, analysis and sound quality have been published. As most of this previous research uses or relies on frequency response curves of a guitar, attention will be paid to the meaning of those curves. Subsequently a model is introduced which is able to capture the most important characteristics of a frequency response curve by using around a dozen parameters.

In Part 2 a finite element model is developed in order to model the sound pressure levels generated by a wooden plate driven by an electrodynamic shaker. As this finite element model will be used for optimization purposes, it makes sense to approximate the physical behaviour of a guitar with a computationally cheap model. Mesh refinement studies are performed to investigate if the number of degrees of freedom can be reduced without sacrificing the quality of the results. Multiple ways of solving the finite element model are available of which two of them are studied. Finally, a more complex geometry is introduced which represents the top plate of an acoustic guitar.

Part 3 presents an algorithm which optimizes the dynamic response of the finite element model to a desired target response, while making use of the model developed in Part 2. Based on the results of the optimization procedure the research questions can be answered, and recommendations for further research are made.

Part I
Literature review and analytical modelling

2 Literature study

2.1 Modelling

Many research has been done on the dynamic behaviour of an acoustic guitar. In general, a dynamic shaker or impact hammer is used to obtain a graph of the frequency response of a guitar, whereafter a numerical model is developed which describes the behaviour of the guitar. Figure 3 shows an example of a frequency response curve. The guitar is excited with a shaker at the location where the strings are attached to the body. The horizontal axis of the plot shows the frequency range of the shaker, while the vertical axis shows the sound pressure level (SPL) measured at some fixed distance, usually 1 meter.

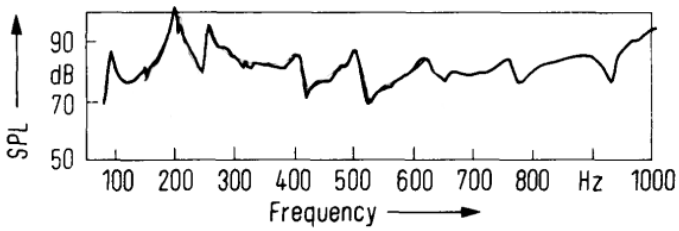

Figure 3: Example of a frequency response curve. Figure is copied from [7].

The first resonance in the frequency response plots always belongs to the Helmholtz resonance of the closed guitar box. It is shown that below this resonance the sound radiated from the soundhole and from the top plate are out of phase, while between the first and second resonance they enhance each other [4].

The second resonance in the frequency response plots is mainly caused by the top plate fundamental resonance. A simple model exists which uses a system of two coupled oscillators based on the Newtonian equations of motion to model both the SPL and the top plate mobility level [5]. Figure 4 depicts a schematic overview of this model. The parameters of the model are determined experimentally. Depending on the system properties, the behaviour of the guitar can be described within a few decibels up to a frequency of about 240 Hz. The equations of motion of such a system are given by

$$\begin{aligned} m_p\ddot{x}_p &= F - k_p x_p - R_p\dot{x}_p + A\Delta p \\ m_a\ddot{x}_a &= S\Delta p - R_a\dot{x}_a \,, \end{aligned} \tag{1}$$

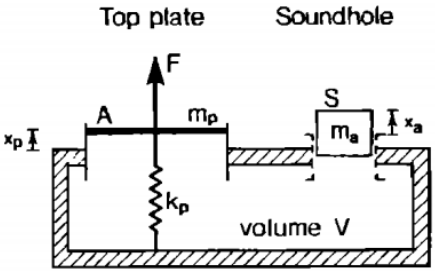

Figure 4: Simplified model for guitar function at low frequencies. This figure is copied from [5].

where the position of the top plate is denoted by x_p, while the position of the air column in the soundhole is denoted by x_a. Both degrees of freedom have an effective mass of m_p and m_a. A and S are the effective areas of the top plate and the sound hole. The resistance to motion is denoted by R_p and R_a. The stiffness of the top plate is k_p, and F is an external force. Changes in pressure can be expressed as a function of those variables as stated in Equation 2. In this equation, c is the

sound velocity in air, ρ the density of air and V the volume of the guitar soundbox. The compression and expansion are assumed to be adiabatic.

$$\Delta p = -\frac{c^2 \rho}{V}(x_p A + x_a S) \tag{2}$$

The two degree of freedom model is extended to three degrees of freedom by adding the motion of the back plate [6]. More recently this model was expanded to four degrees of freedom by including the dynamics of the sides [8]. However, this seems an unnecessary complication as the dynamics of the sides cannot be accurately described by just one variable [9].

All of the research mentioned above was aimed at classical guitars. Those guitars have nylon strings, while guitars with steel strings are called western guitars. Western guitars have different sizes and bracing arrangements. Because of this the frequency response of classical and western guitars is very different. However, it is shown that the two degree of freedom model is also applicable to western guitars [11].

An interesting application of the two degree of freedom model is described in [10]. In this research the gradients of the model's eigenfrequencies, with respect to the input parameters, are obtained by a sensitivity analysis. However, only for a few of the input parameters it is known how to implement their theoretical changes in the physical model.

Another approach of modelling the SPL of an acoustic guitar is presented by Ove Christensen [7] in his paper *An Oscillator Model for Analysis of Guitar Sound Pressure Response* (1984). The method described in this research uses a few uncoupled oscillators, each characterized by its resonance frequency and Q-value, together with the ratio of its effective piston area to effective mass as seen from the driving point. The behaviour of any guitar in the frequency range from 150 to 600 Hz can be very well described by this oscillator model. Chapter 4 will explain the oscillator model in more detail.

2.2 Sound quality

In general humans can distinguish changes of 3 dB in sound pressure level, which is known as the just-noticeable difference [42]. However this is very dependent on the type of sound to which the listener is exposed. For example, values of 1 dB are also found in literature [43].
Psychoacoustic listening tests indicate that the perceived sound quality of an acoustic guitar is mainly determined by its dynamical behaviour below 1000 Hz, and also a correlation was found between the perceived sound quality and retail prices of guitars [21].

2.3 Optimization

Previous research has been performed on optimization of sound producing structures, for example the optimization of a bell [27]. After a bell is hit by a clapper it starts to vibrate at its eigenfrequencies. Depending on the ratio between the frequencies the sound can be perceived as major or minor. In this study those eigenfrequencies were optimized using the finite element method and the boundary element method. The axisymmetric shape of a bell enabled it to be modelled with a two-dimensional model instead of three-dimensional.

Recently a study was published which uses operating deflection shape analysis to optimize the response of a guitar [28]. As far as known this is the first study which applies optimization algorithms it the field of guitar design. An experimental setup modelled the top plate of a guitar as a rectangular acrylic plate with braces. For a single frequency the response was optimized by changing the shape of the braces, using a nonlinear programming algorithm. The usefulness of this approach is questionable as, due to both the string harmonics and the presence of multiple strings, a real guitar is always excited at multiple frequencies.

3 Frequency response curves

A lot of the research mentioned in the literature study uses or relies on frequency response curves. Surprisingly, very little is written about the meaning of those curves and how to use them. As it is important to know what is actually measured and how this translates to practice, this chapter will be focused on the meaning of the frequency response curves.

3.1 Obtaining a frequency response curve

An electrodynamic shaker is attached to the guitar which excites the structure with a 1 Newton sinusoidal varying force throughout a chosen frequency range. The shaker is located between the third and fourth string. Its force is directed perpendicular to the guitar's top plate as shown by the blue arrow in Figure 5.

Mind that a guitar being played is exposed to different kind of excitations than the excitation used to obtain a frequency response curve. The main difference is that the guitar's string force acts parallel to the top plate instead of perpendicular. As there is a distance between the string and the top plate, the string force also causes a bending moment. The red arrows in Figure 5 indicate the directions of the string forces. It is important to realize that because of those differences some design changes might result in a smaller or larger change in sound than the frequency response curve suggests.

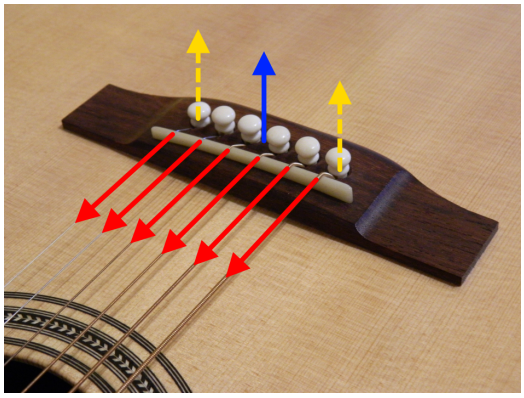

Figure 5: Force directions.

Figure 6 depicts the four lowest eigenmodes of a classical guitar its top plate. Blank and shaded areas move in opposite phase. The eigenmodes are named T(1,1), T(2,1) etc. The first number indicates the number of anti-nodal points in horizontal direction, the second number indicates the number of anti-nodal points in vertical direction.

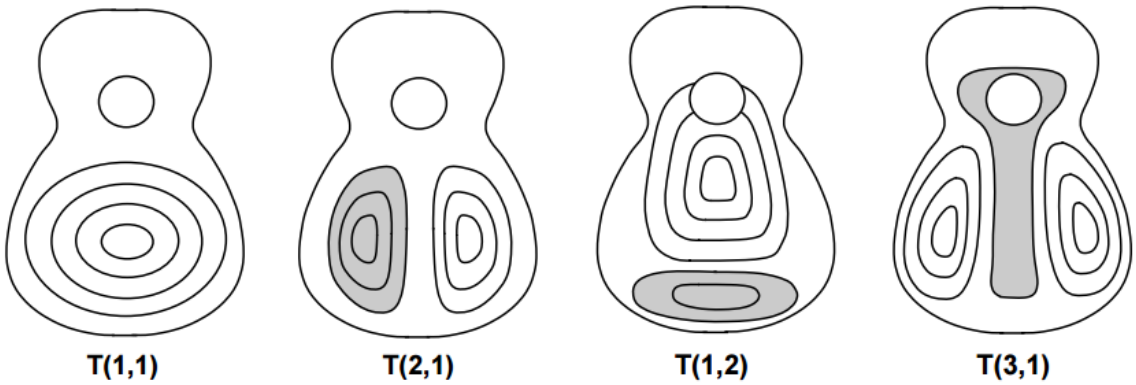

Figure 6: Lowest eigenmodes of the top plate. Figure is copied from [12].

Suppose that the T(2,1) mode is completely symmetric. From the distance where the instrument could be considered as a point source of sound this eigenmode would not contribute to the sound pressure level, as it does not cause any net volume displacement of the air. But the internal structure of the guitar usually is not completely symmetrical, neither are the material properties. Although, this example illustrates it is important to realize that it is not the total volume displacement of air which is a measure for the generated sound, but the net volume displacement.

The relative presence of an eigenmode in the frequency response curve depends, among other things, on its effective modal mass. The effective modal mass is influenced by the location of the driving point [33]. One could imagine that the effective modal mass of the T(2,1) mode is much higher for the blue arrow in Figure 5 than it would be for one of the yellow arrows for example, as the blue arrow is located closer to a nodal line. Although most of the previous research does not pay a lot of attention to the location of the driving point when measuring frequency responses, it is confirmed by [12] that those locations can have quite some influence on the obtained curve.

3.2 String excitation frequencies

The frequency of a string is always denoted by just one value, which is the first eigenfrequency of the string. When a string is plucked higher eigenmodes are also excited [26]. The frequencies belonging to those higher modes (harmonics) are multiples of the string's first eigenfrequency.[1] Figure 7 shows the six lowest eigenmodes of a string. The ratio between the magnitude of the excited eigenmodes depends on the location on the string where it is plucked.

A frequency response curve of a random guitar is depicted in Figure 8. Suppose this guitar is excited by a string tuned at a frequency of 147 Hz. The vertical lines in the frequency response curve denote the frequencies of the string harmonics. The eigenmodes of the construction are excited with certain force amplitudes at those frequencies, resulting in the overall sound. In general, the excitation force caused by a plucked string decreases as the number of the string's eigenmode increases.

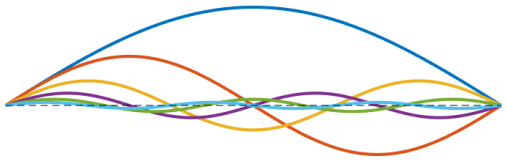

Figure 7: Eigenmodes of a string.

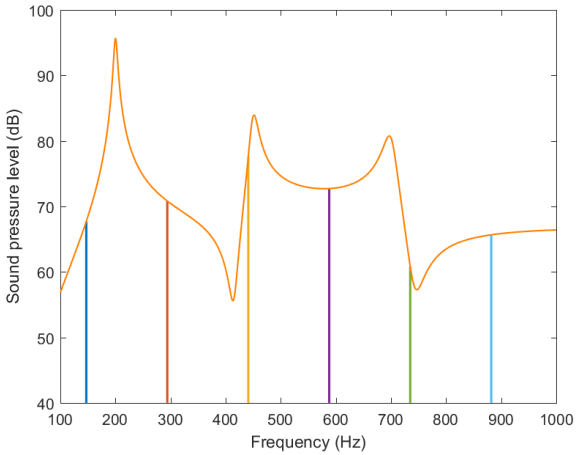

Figure 8: String excitation frequencies.

[1] Theoretically those harmonics are exact multiples of the eigenmodes. Opposed to theoretical string models, real strings do obtain a small bending stiffness. Consequently the frequencies belonging to the string harmonics are slightly different from the exact multiples of the base frequency.

3.3 Damping

When a guitar is played, the sound perceived by a listener over time is related to the transient response of the instrument. The sharpness of the peaks in the frequency response curves indicate the amount of damping present for the concerning eigenmodes. Figure 9 depicts the frequency response of a system for two different damping values, everything else being equal.
Impulse responses can be used to compare the transient behaviour of systems [30]. As an example, in Figure 10 the qualitative effect of different damping values is made more visual by an impulse response curve.

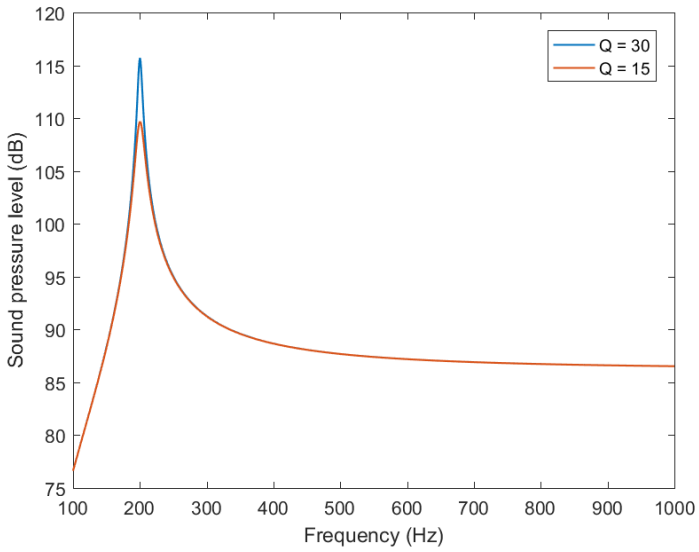

Figure 9: Frequency response of a single oscillator.

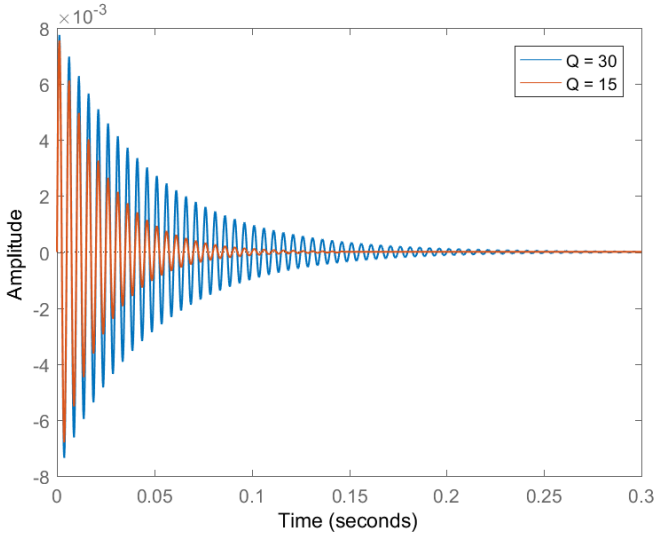

Figure 10: Impulse response of a single oscillator.

4 An oscillator model of the acoustic guitar

A disk vibrating in air will generate pressure changes, which can be converted to a sound pressure level (SPL). It is shown by Christensen [7] that for a certain frequency range the SPL generated by a guitar can be approximated by the SPL generated by three to five vibrating oscillators. Each oscillator is characterized by its resonance frequency and Q-value, together with the ratio of its effective piston area to equivalent mass as seen from the driving point.

Firstly a theoretical background is presented in this chapter which shows how to calculate the sound pressure level generated by a vibrating disk. Next, it is explained how to obtain a frequency response curve from arbitrary chosen parameter values for the oscillator model. Also the reader will be given some insight in the consequences of some parameter choices, such as a negative effective area. The main goal of this chapter is to show that it is possible to give quantitative descriptions of a guitar's dynamical response, instead of only qualitative subjective descriptions from listeners.

Figure 11 depicts the frequency response curves of five different guitars, along with their fitted response curves according to the oscillator model. It shows that for a certain frequency range this model is indeed able to give an approximation of the sound pressure level. It also confirms the oscillator model does not take into account the first resonance peak, which is caused by the Helmholtz resonance as described in Chapter 2.

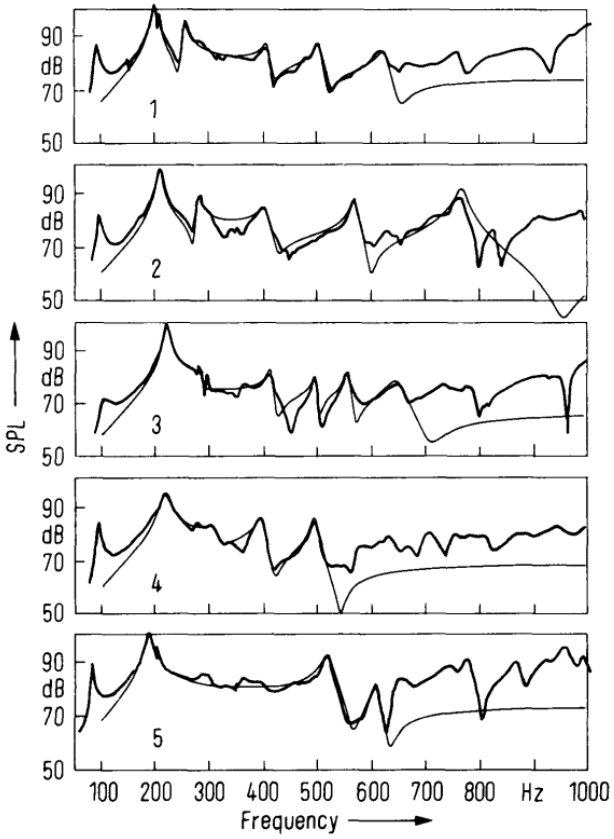

Figure 11: Comparison between measured sound pressure level responses (thin lines) and calculated ones (heavy lines) for five guitars. This figure is copied from [7].

4.1 Sound pressure level generated by a vibrating disk

The sound pressure created by a plane radiator such as a vibrating disk is given by

$$p = -\frac{i\omega\rho}{2\pi r}\, q\, e^{-ikr}, \tag{3}$$

where ρ is the density of the surrounding fluid (air), r the distance from the sound source and q the volume velocity [31]. The volume velocity equals the surface area A multiplied by the velocity u of the disk:

$$q = uA. \tag{4}$$

Equation 4 is valid for a disk which has a homogeneous displacement. If the disk deforms during the motion, the velocity is not equal all over the surface. In this case the volume velocity is obtained by integrating the velocity over the surface:

$$q = \int u_i(x, y)\, da. \tag{5}$$

The last term of Equation 3 introduces the phase behaviour. When converting a sound pressure to SPL the phase information is dropped, which means this term could be omitted.
The SPL caused by a complex sound pressure equals:

$$\mathrm{SPL} = 10 \log_{10} \left(\frac{(p^2)_{av}}{(p_{ref})^2} \right). \tag{6}$$

A reference pressure p_{ref} of $2 \cdot 10^{-5} Pa$ is used, and $(p^2)_{av}$ is calculated as:

$$(p^2)_{av} = \frac{1}{2} \left(\mathrm{Re}(p)^2 + \mathrm{Im}(p)^2 \right). \tag{7}$$

In Chapter 5 the sound pressure level generated by a vibrating disk is studied using a finite element model. For some cases, analytical approximations as presented above are available which will be used to verify the model.

4.2 Dynamics of an oscillator

The mass, area, eigenfrequency and quality factor are the input parameters for each oscillator. Throughout this research a sinusoidally varying force of 1 Newton is applied as an external force. Classical theories for vibration analysis are used to obtain the velocity of the oscillator [32]:

$$u = \frac{F}{m} \frac{i\omega}{(\omega_0^2 - \omega^2) + i\gamma\omega}. \tag{8}$$

Both the velocity and area of the oscillator are substituted into Equation 4 in order to obtain its sound pressure response at a chosen excitation frequency. The sound pressure's magnitude can now be written as:

$$p = F \frac{A}{m} \frac{\rho}{4\pi r} \frac{\omega^2}{(\omega_0^2 - \omega^2) + i\gamma\omega}. \tag{9}$$

If this calculation is performed for a range of frequencies and the sound pressure is converted to SPL a frequency response curve is obtained, as was shown in Figure 9 on page 16 for some arbitrary input parameters.

4.3 Dynamics of a system of oscillators

Figure 12 shows four frequency response curves generated with the oscillator model. Except for the sign of the area of the second and third oscillator, the same input parameters are used for all curves.

Although a negative surface area might be difficult to imagine, this can be clarified by Figure 13. If the grey part of for example the T(1,2) mode would cause a larger volume velocity than the blank part, the net volume velocity of this eigenmode will have an opposite sign compared to the first eigenmode's volume velocity.

The frequency response curves show that depending on the sign of the area an anti-resonance may occur. In the frequency range surrounding them those anti-resonances have a big impact on the SPL. The behaviour of a guitar's vibrating top plate shows a lot of parallels with motion systems containing multiple eigenmodes. This is a general class of systems for which techniques are available to analyse them, such as described in [33]. Those techniques provide a lot of insight in understanding the effect of parameter changes on the oscillator model.

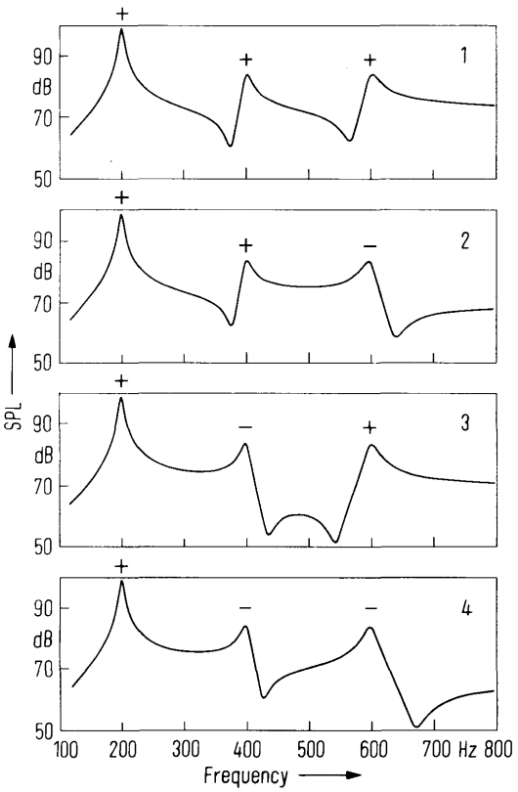

Figure 12: The plus and minus signs indicate the sign of the surface area, all other parameter values are equal. This figure is copied from [7].

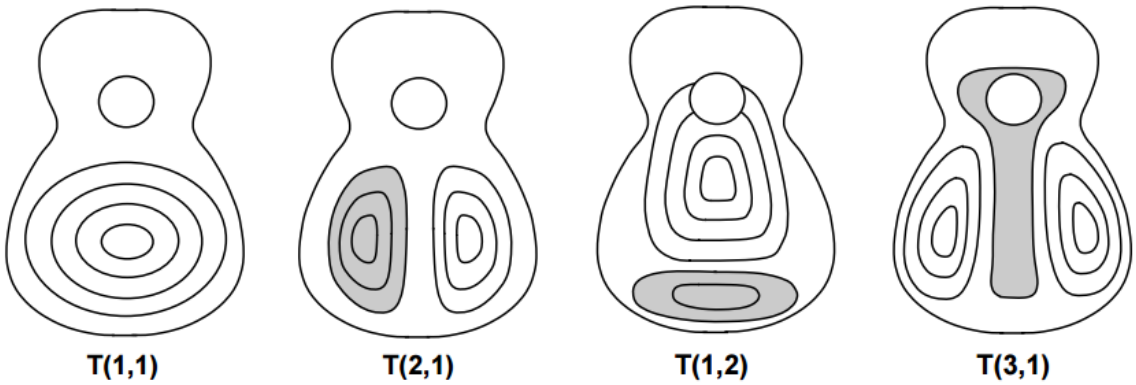

Figure 13: Lowest eigenmodes of the top plate. Figure is copied from [12].

Part II
Numerical model of the top plate

5 Finite element modelling of the sound pressure level

In this chapter a finite element model is introduced in order to model the sound pressure levels generated by a wooden disk driven by an electrodynamic shaker for a range of excitation frequencies. An extended version of the model will be used later in this research, which enables the user to predict the effects of design variable and material property variations on sound pressure levels generated by a guitar. The analytical formulation which describes the sound pressure levels generated by a vibrating disk, as presented in the previous chapter, will be used to partly verify the finite element model.

5.1 Theory

The finite element method subdivides a geometry in small domains named *elements*. Elements contain *nodes*, this are points which enable the element to interact with the surroundings. In structural mechanics this interaction consists of forces and displacements. Forces can be induced by neighbouring elements, body loads (for example gravity forces) or other causes from the outside. Displacements are typically only imposed from the outside environment as a boundary condition. A geometry subdivided in those elements is called a *mesh*. Together with the boundary conditions the mesh is used to translate the properties of the geometry and the material to a mass, damping and stiffness matrix, usually denoted by $\mathbf{M}$, $\mathbf{C}$ and $\mathbf{K}$. The displacement, velocity and acceleration of all individual nodes can be obtained by solving the equilibrium equation set up by those matrices. For more information on finite element modelling in general we would like to forward the reader to other literature available on this subject [32][34].

The size of the matrices depends on the problem one wants to solve. In general those problems are too large to solve by hand, the number of degrees of freedom present in the models described in this report for example vary from several thousands up to 300,000. Specialized software packages are available (Abaqus FEA, ANSYS, COMSOL) which build the system matrices and solve the equilibrium equation from the input given by the user. More information about the software used in this research is available in A.1.

Equilibrium equation

The distribution of the pressure throughout the air domain is described by the Helmholtz equation [41]:

$$\frac{\partial^2 p}{\partial t^2} = c^2 \Delta p, \tag{10}$$

where p is the air pressure and c the speed of sound in air. After discretization of both the structural mechanics domain and the pressure domain, the obtained equilibrium equation is in this form:

$$\begin{bmatrix} \mathbf{M}_{ss} & 0 \\ \mathbf{M}_{sp} & \mathbf{M}_{pp} \end{bmatrix} \begin{bmatrix} \ddot{\mathbf{x}}_s \\ \ddot{\mathbf{x}}_p \end{bmatrix} + \begin{bmatrix} \mathbf{C}_{ss} & 0 \\ 0 & \mathbf{C}_{pp} \end{bmatrix} \begin{bmatrix} \dot{\mathbf{x}}_s \\ \dot{\mathbf{x}}_p \end{bmatrix} + \begin{bmatrix} \mathbf{K}_{ss} & \mathbf{K}_{ps} \\ 0 & \mathbf{K}_{pp} \end{bmatrix} \begin{bmatrix} \mathbf{x}_s \\ \mathbf{x}_p \end{bmatrix} = \begin{bmatrix} \mathbf{F}_s \\ 0 \end{bmatrix}. \tag{11}$$

The terms containing subscript s or ss completely belong to the structural domain, while the terms containing subscript p or pp completely belong to the pressure domain. It is seen that both the mass matrix and the stiffness matrix contain an off-diagonal term, $\mathbf{M}_{sp}$ and $\mathbf{K}_{ps}$, which contain information about the coupling between the structural domain and the pressure domain. It can be shown that $\mathbf{M}_{sp} = -\rho \mathbf{K}_{ps}^T$, where ρ is the air mass density [34]. The term $\mathbf{F_s}$ contains the external force as imposed by the shaker.

5.2 Geometry, materials and mesh

Geometry

A wooden disk is located at the center of a coordinate system, surrounded by a sphere filled with air. This is shown in Figure 14. Depending on the type of analysis the air is not present in all cases described in this research.

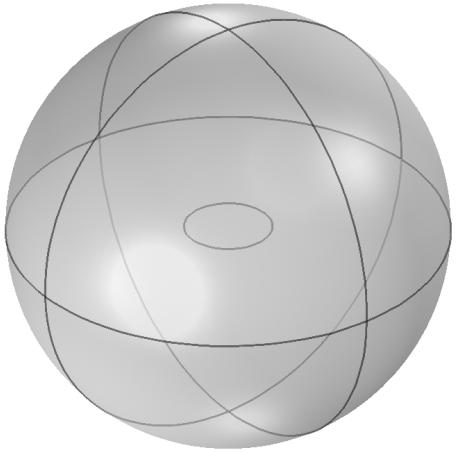

Figure 14: Geometry of the wooden disk surrounded by a sphere filled with air

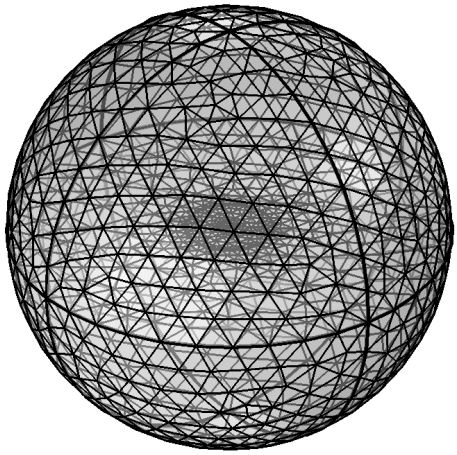

Figure 15: Mesh of the domain

Materials

Two materials will be used in this research; air and spruce. The material properties of air are listed in Table 1. Unless stated different, the material properties of the wood are as listed in Table 2.

	Air
Density ρ	1.2044 kg/m^3
Speed of sound c	343 m/s

Table 1: Material properties of air

	Spruce
Density ρ	450 kg/m^3
Young's modulus E	7.5 GPa
Poisson's ratio ν	0.33
Isotropic structural loss factor η_s	0.04

Table 2: Material properties of wood

Mesh

Although the thickness of the wooden disk is much smaller than its other dimensions, initially three-dimensional tetrahedral elements are used instead of two-dimensional plate elements. Plate bending theory assumes some simplifications compared to bending of a tetrahedral element which might decrease the reliability of the model [34]. Both the air and wood domain are meshed with quadratic tetrahedral elements. A mesh of the air domain is shown in Figure 15. In Chapter 6 and 7 mesh refinement studies are performed. During this study it will be investigated if the simplifications of the two-dimensional elements are allowable. Based on the results it is decided whether two-dimensional or three-dimensional elements are used in the final guitar model.

5.3 Boundary conditions

Depending on whether the disk is a shell (flat) or a solid (extrusion), the edges or sides of it are fixed. A frequency dependent point load of 1 Newton is applied perpendicular to the disk at its center. The horizontal axes of the frequency response curves shown in this report represent the sinusoidally varying frequency of the force. It is chosen to model the force as a point load as during physical experiments usually a dynamic shaker or testing hammer is used. It seems a valid approximation to model their excited force with a point load instead of for example a distributed load.

Acoustic boundary conditions

The COMSOL Acoustics Module enables the user to set up boundary conditions on surfaces involved in the calculation of the sound pressure. Three boundary conditions are used for this, of which the equations are listed in A.2. The boundary condition on the surface of the sphere is a 'Spherical wave radiation' condition. The sphere is cut in half by an horizontal plane called the 'Interior sound hard boundary'. A hole is removed from this plane, in which the disk is positioned. The surface of the moving disk is defined as an 'Acoustic-structure boundary'. Figure 16 clarifies the locations of the surfaces.

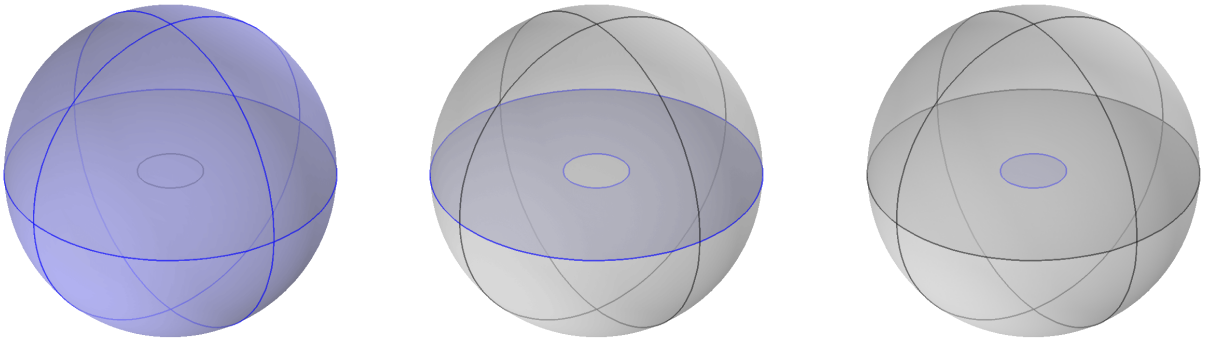

(a) Spherical wave radiation (b) Interior sound hard boundary (c) Acoustic-structure boundary

Figure 16: Surface boundary conditions

The spherical wave radiation condition models a non-reflecting open boundary, which simulates an infinite space. It ignores the tangential components of the acoustic field at the boundary.
The interior sound hard boundary acts as a wall. This is denoted by

$$\mathbf{n} \cdot \nabla p_{\mathrm{t}} = 0, \tag{12}$$

where $\mathbf{n}$ is the normal vector to the boundary surface and ∇p_{t} the gradient of the air pressure at the boundary. This gradient is proportional to the air velocity, which of course equals zero at a stationary wall. The acoustic-structure boundary couples the pressure domain and the structural mechanics domain. On this boundary the normal component of the air velocity equals the normal component of the structure's velocity $\mathbf{u}_{\mathrm{tt}}$:

$$\mathbf{n} \cdot \frac{1}{\rho_{\mathrm{c}}} \nabla p_{\mathrm{t}} = \mathbf{n} \cdot \mathbf{u}_{\mathrm{tt}}. \tag{13}$$

5.4 Verification

Imposed rigid body displacement

Chapter 4 presented an analytical approach to obtain the sound pressure level generated by a vibrating disk. This approach will be used to verify the implementation of the acoustic-structure boundary and the simulated pressure in the air domain. Unlike explained before, in this subsection instead of a force a rigid body vibration is imposed on the disk. The edges of the disk are not fixed as this would obstruct rigid body motion.

For a disk having a radius of 0.2 meter and a displacement amplitude of 0.1 millimeter, the simulated sound pressure at 1 meter distance is shown in Figure 17. The analytical solution from Equation 6 is also plotted in this figure. It is seen that the results of the finite element model correspond with the analytical solution, even though the analytical solution is only an approximation as the sound source is considered to be a point instead of a surface.

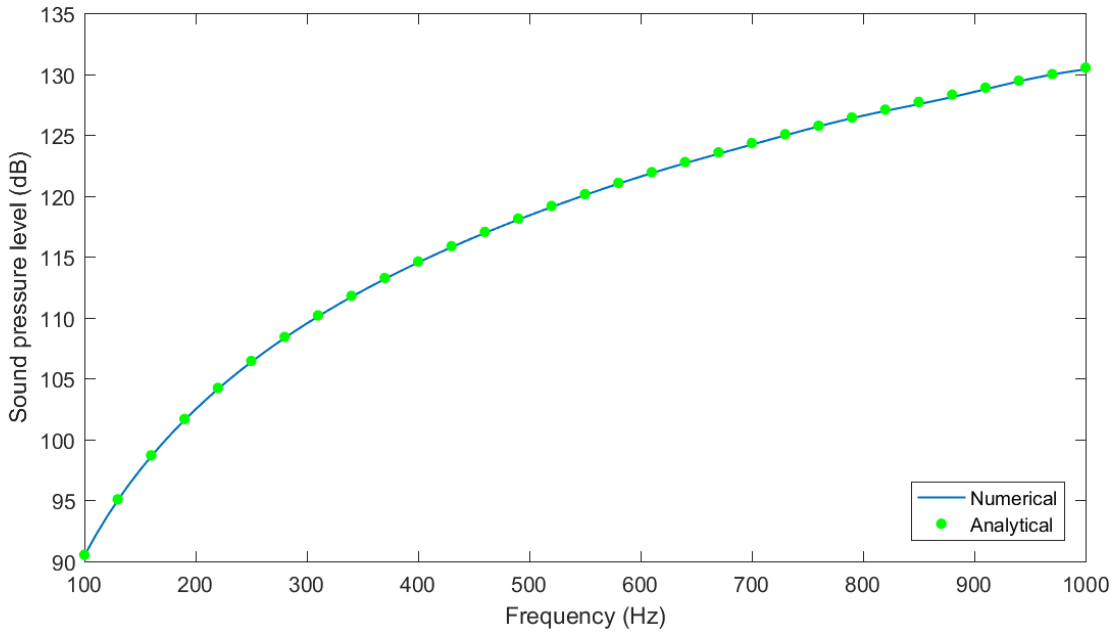

Figure 17: The acoustic domain of the numerical model is verified by calculating the SPL at 1 meter distance analytically for a disk undergoing rigid body vibrations.

Imposed load

The previous subsection was about the sound pressure generated by a vibrating rigid disk undergoing an imposed maximum displacement. In this subsection, the edge of the disk is clamped again while the center is excited with a sinusoidally varying force of 1 Newton. As the disk is not rigid anymore the generated sound pressure is affected by the structural dynamics of the disk.

Figure 18 shows the six lowest eigenmodes of a circular plate. The listed frequencies are the eigenfrequencies of the plate if it would not be surrounded by air. Eigenmodes two to five are not excited by a force applied at the plate's center. This is confirmed by Figure 19, which shows the SPL at 1 meter distance. Vertical lines are drawn at the above-mentioned eigenfrequencies of the plate. The resonance peaks of the SPL appear at lower frequencies than those eigenfrequencies. This is caused by the interaction between the disk and the air surrounding it, which lowers the eigenfrequencies as a result of the added mass effect [41].

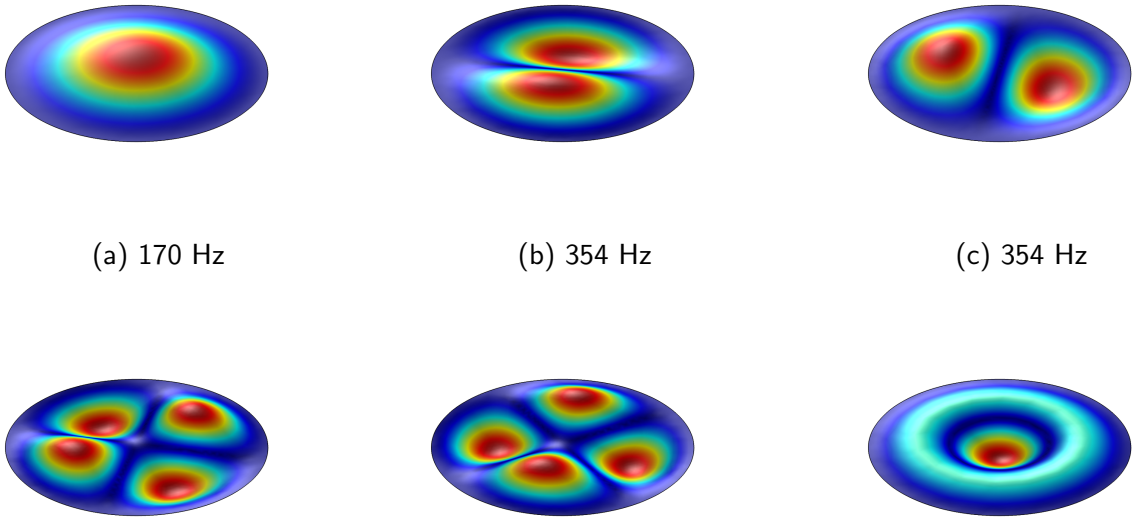

(a) 170 Hz (b) 354 Hz (c) 354 Hz

(d) 581 Hz (e) 581 Hz (f) 662 Hz

Figure 18: Six lowest eigenmodes of a circular plate.

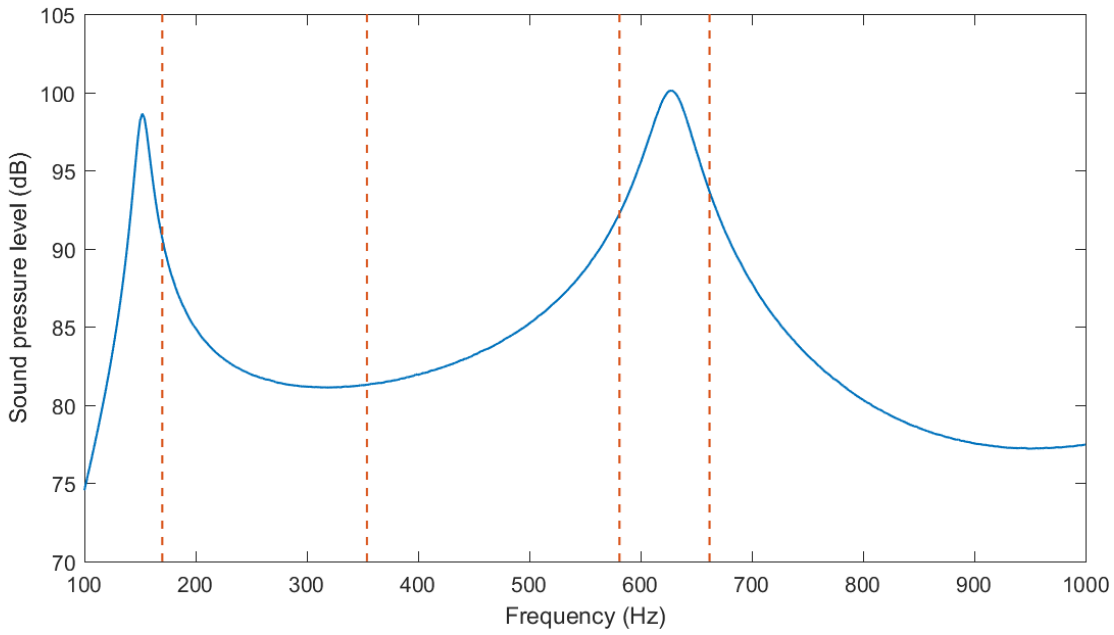

Figure 19: SPL caused by a sinusoidally varying force acting on the clamped disk surrounded by air. The vertical lines indicate the eigenfrequencies of the disk if no air would be present.

Verification of the stiffness matrix

An analytical solution exists to calculate the maximum displacement of a clamped circular plate subjected to a static load [36]. The maximum displacement calculated by the finite element model at frequencies far below the first eigenfrequency should approximately be equal to this. In A.3 for both situations the maximum displacement is obtained. Both situations neglect the added mass effect caused by the air surrounding the plate. The difference between the maximum displacement of the static, analytical solution and the finite element model excited at a frequency of 1 Hertz is 2%. Based on this, it can be concluded that the stiffness matrix of the finite element model accurately describes the stiffness of the real system.

Verification of the eigenfrequencies

The eigenfrequencies of a clamped circular plate can be obtained analytically [37]. A few of them are listed in Table 3, which shows that the difference between the eigenfrequencies obtained by the finite element model and the ones obtained analytically is very small. Based on this, it can be concluded that next to the stiffness matrix also the mass matrix of the finite element model accurately describes the real system.

Eigenmode	FE model (Hz)	Analytical (Hz)
1	170	170
2-3	354	355
6	662	664

Table 3: Verification of the eigenfrequencies

5.5 Assumption of the disk being a point source

As previously stated, the analytical solution assumes that the disk behaves like a point source of sound. Figure 20 shows that this assumption is also valid for measurement distances less than a meter. Of course this depends on the size of the disk; increasing the size will increase the minimum distance from where it is possible to model the disk as a point source. A disk radius of 0.2 meter is used, which results in a surface area about twice as large as the equivalent surface areas of eigenmodes of the guitar found in literature [12]. The overlap of the lines in Figure 20 at measurement distances above 0.3 meter indicates the point source assumption is valid. The uniform pressure distribution on the surface of the 1-meter radius sphere shown in Figure 21 also confirms that the disk can be considered as a point source. For this figure an excitation frequency of 100 Hz was applied.
It can be concluded that for measurements of an acoustic guitar a measurement distance of 1 meter is sufficiently large to be able to consider the guitar as a point source of sound.

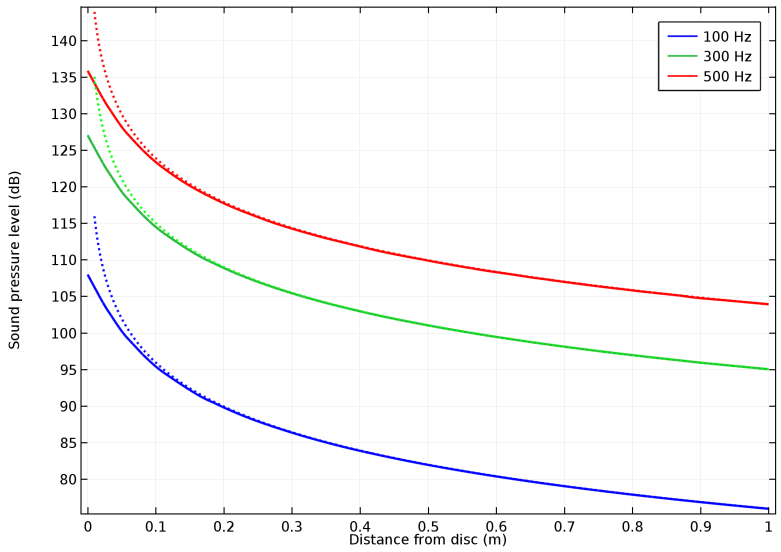

Figure 20: Simulation (solid lines) versus analytical solution (dotted lines)

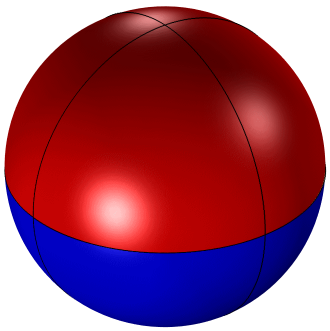

Figure 21: Pressure distribution at the sphere's surface area for an excitation frequency of 100 Hz. The uniform distribution confirms the validity of the point source assumption.

5.6 Solver

The frequency responses of the structures presented in this research are usually obtained for a wide range of frequencies. For problems which have to be solved for a range of frequencies it makes sense to use a modal solver. One of the features of this approach is the possibility of applying modal truncation, which decreases the computational cost incredibly compared to the direct method of solving the equilibrium equation.
But unfortunately the physics of the pressure domain and the structural mechanics domain are coupled, and a modal approach cannot be implemented if the model includes coupled physics. In Chapter 6 it is shown that the coupling between the air and the structure is too large to be neglected. For the reason explained above the equilibrium equation is solved by a direct method. This means that the computational cost of obtaining a frequency response curve is proportional to the number of function evaluations needed in order to obtain a smooth, linearly interpolated curve from a discrete set of points.

6 Mesh refinement study of the air domain

The model developed in this research will be used within an optimization algorithm, which rises the desire to have a computationally cheap model. The goal of a mesh refinement study is to decrease the number of degrees of freedom of the model while not compromising the accuracy of the results. At this stage we will not perform a mesh refinement study on the disk yet as, opposed to the air, the geometry of the disk is not representable for the geometry used later in this research. Although, in a later stage a mesh refinement study of the wooden parts will also be performed in order to be able to achieve an optimization process which is as cost effective as possible.

The frequency band for all analyses performed in this research starts at 100 Hz and ends at 1000 Hz. In the literature study it was explained that below 100 Hz the response of a guitar is mainly determined by the soundbox instead of its top plate. As the model used in this research does not include the soundbox, frequencies below 100 Hz are not considered. It was also shown in the literature study that the perceived sound quality of an acoustic guitar is mainly determined by its response below 1000 Hz, which explains the upper limit for the frequency band of interest.

6.1 Size of the air elements

As a rule of thumb, by using quadratic elements a minimum of five elements per wavelength should be used initially [35]. Depending on the type of problem one wants to solve and the desired accuracy of the solution it is possible that less number of elements per wavelength will be sufficient. A mesh refinement study is performed which calculates the SPL by using five different maximum element sizes for the air domain. The results are plotted in Figure 22, e denotes the minimum number of elements per wavelength. Note that the wavelength is a function of the frequency, which means that the geometry is remeshed for every data point. Figure 23 shows the number of degrees of freedom present in the air domain. Mean difference, standard deviation and maximal difference of all SPL-curves presented in this mesh refinement study are listed in A.4.

The green curve is assumed to be the most accurate solution as it uses the finest mesh. As one would expect it is observed that, starting with a coarse mesh, the other curves converge to this green curve for decreasing element sizes. It also is observed that by using a minimum number of only one element per wavelength, there is a considerable inaccuracy in both the frequencies between 400-500 Hertz and above 600 Hertz. A mesh containing at least two elements per wavelength does show less inaccuracies in the high frequency range, while between 400 and 500 Hertz it still shows a noticeable difference with the most accurate solution. It seems that a mesh containing a minimum number of three elements per wavelength is not far off from the desired solution. Considering the rapidly increasing number of degrees of freedom for finer meshes while the gain in accuracy is limited, it is concluded that the air domain should be meshed with a minimum number of three elements per wavelength.

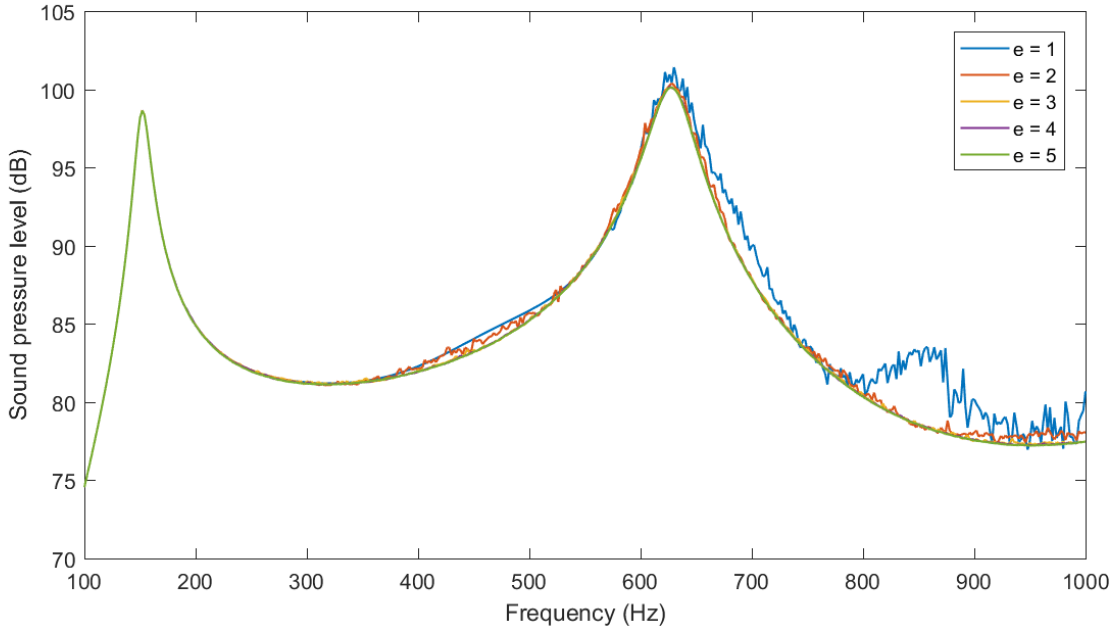

Figure 22: SPL as calculated by using several minimum numbers of elements per wavelength e

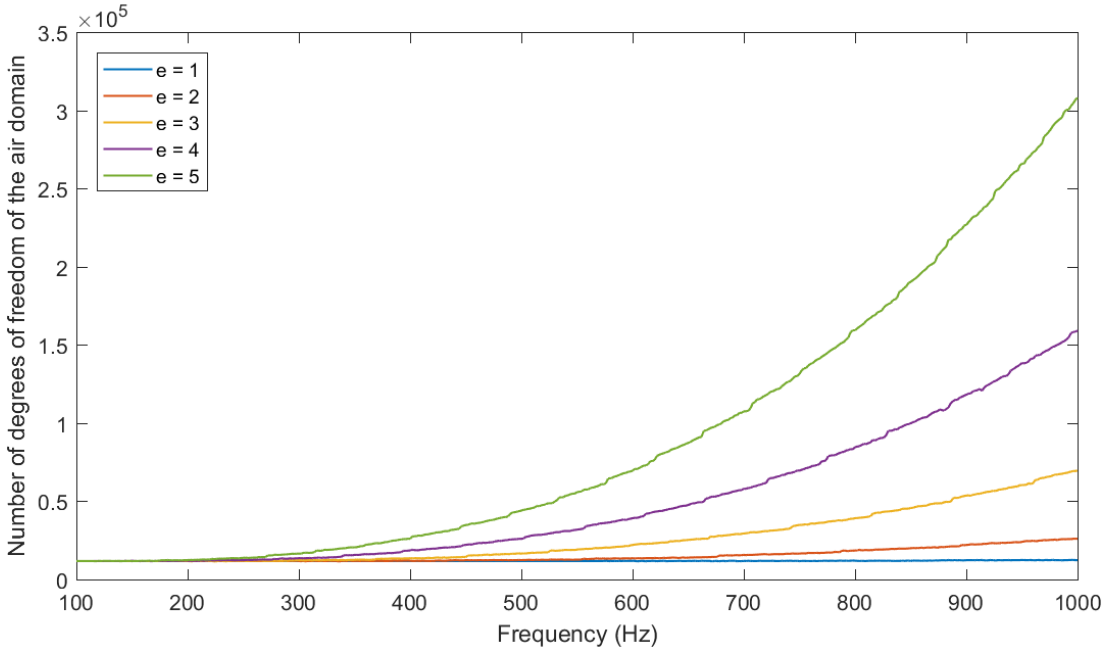

Figure 23: Number of DOF of the air domain for using different element sizes

6.2 Calculating SPL directly from velocity field

The vibrating surface of the disk causes pressure changes in the air surrounding it. In the previous section the SPL was measured at 1 meter distance in the finite element model, which solves the way the pressure changes are distributed throughout the air domain. In this section we will show that the SPL can also be calculated more directly from the velocity field of the vibrating surface. We will call this the semi-analytical solution.

Equation 14 describes how the volume velocity of the vibrating disk is obtained; it equals the velocity field integrated over the surface area of the disk. The result of this can be used in an analytical formulation to calculate the SPL caused by a point source, as seen in Equation 15. Note that both equations have already been presented in Chapter 4.

$$q = \int u_i(x, y)\, da \tag{14}$$

$$p = -\frac{i\omega\rho}{2\pi r}\, q\, e^{-ikr} \tag{15}$$

Figure 24 shows the difference in SPL between a measurement in the air domain and by applying the semi-analytical approach. For both methods a mesh with a minimum number of five elements per wavelength is used. It is observed that over the frequency range of interest the difference is always less than 0.5 dB.

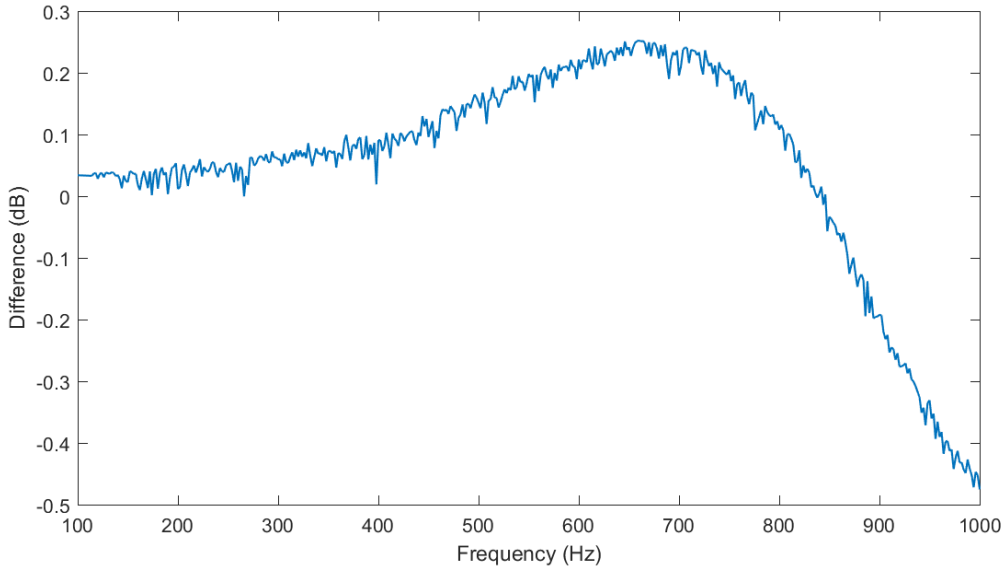

Figure 24: Difference in SPL between measurement and semi-analytical approach.

Unfortunately, this does not mean we can just remove the air surrounding the disk. As described before the vibrating disk causes pressure changes in the air surrounding it. But this coupling acts in two directions; the resistance of the air also reduces the deformation of the disk. While Chapter 5 presented the mathematical description of the coupling, we will now focus on what this actually means for the SPL.

Figure 25 shows what happens to the SPL when the air is removed. It is observed that by removing the air the damping is decreased and the eigenfrequencies are increased. A surface moving trough air with a certain velocity is subjected to damping, which logically disappears if it is not exposed to air anymore during its motion. The increase of the eigenfrequencies can be explained by the fact that a boundary layer of air is set in motion by the vibrating disk. The mass of this layer lowers the eigenfrequencies, which means that removing the air will indeed increase the eigenfrequencies.
If one is able to find a way to model this added mass effect of the air without having to model the air itself, the number of degrees of freedom needed to solve the model can be reduced significantly.

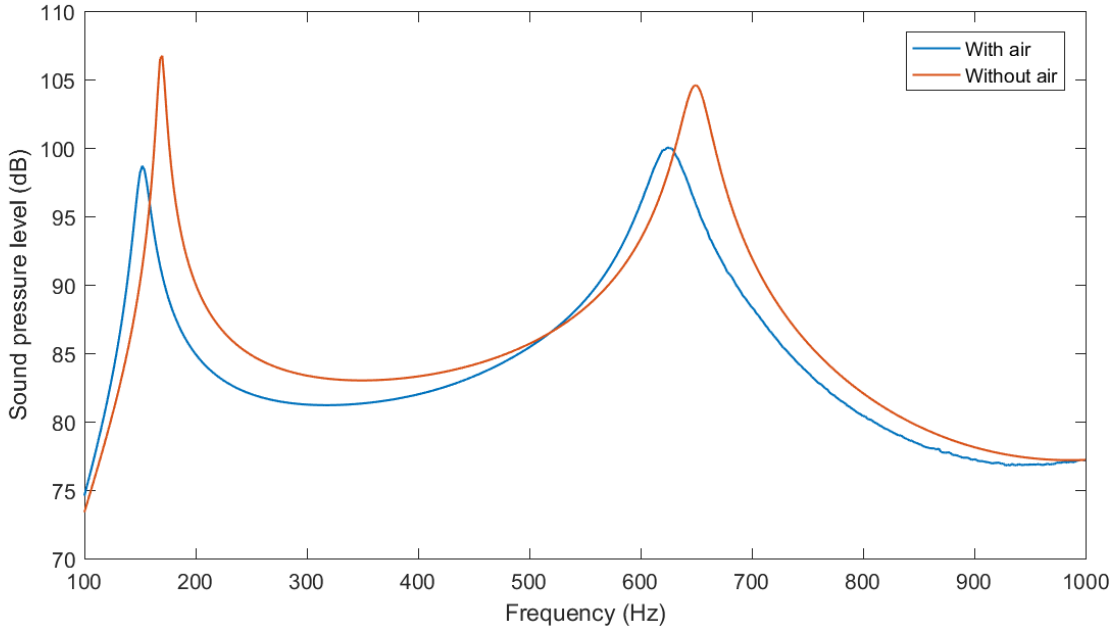

Figure 25: SPL with and without air surrounding the disk.

Fortunately, it appears that another option to decrease the number of degrees of freedom is available. The beginning of this section presented a semi-analytical way of obtaining the SPL. Instead of measuring the SPL itself at 1 meter distance, this method uses the integral of the velocity field of the disk its surface area in order to obtain the SPL.
The yellow curve in Figure 26 shows the SPL as obtained by performing this semi-analytical calculation, while using a mesh with a minimum number of only one element per wavelength. It was already shown that a mesh this coarse is not able to represent the SPL accurately throughout the whole frequency range if it is obtained by measuring at 1 meter distance, which is repeated in Figure 26 by the red and blue line. But by observing this figure, it appears that although such a coarse mesh is not able to accurately represent the sound waves travelling trough the air, the air resistance applied on the disk by a mesh this coarse ís representative.
It turns out that by using the semi-analytical approach the difference in SPL between the computationally most expensive problem (measuring at 1 meter distance for e=5) and the cheapest (semi-analytical calculation for e=1) is at most 0.7 dB, as shown in Figure 27. Based on this example it is decided that a very coarse mesh for the air domain can be used.

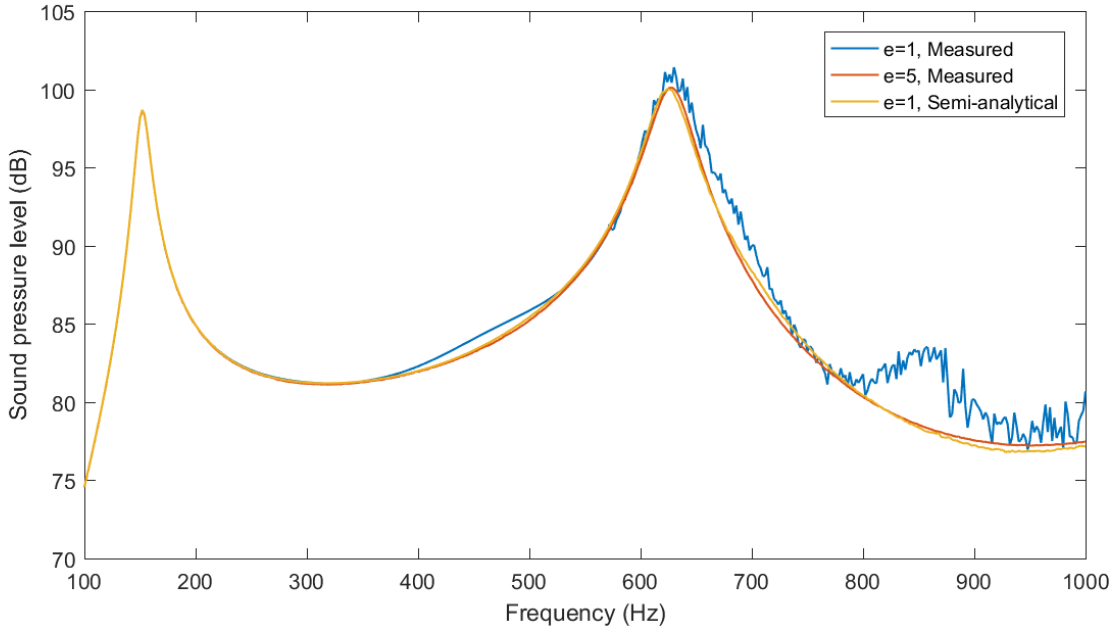

Figure 26: Semi-analytically obtained SPL while using a coarse mesh and measured SPL while using both a coarse and a fine mesh.

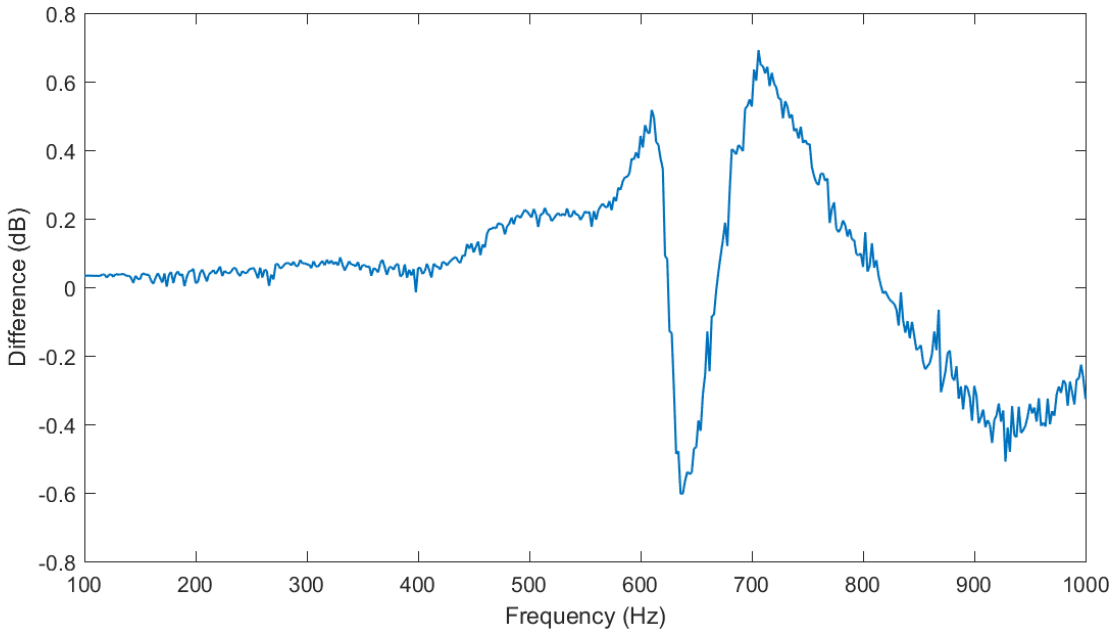

Figure 27: Difference in SPL between measurement with e=5 and semi-analytical approach with e=1.

6.3 Symmetry of the air domain

The sphere containing the air is actually a combination of two halve spheres, which are separated by a sound hard boundary and the wooden disk. As explained before the air adds mass and damping to the wooden structure. The effects on the out-of-plane motion of the wooden structure caused by both of these phenomena are proportional to the air density, and are independent of the direction of the motion [41][38]. This enables one to model only one half of the sphere instead of two if this is compensated by doubling the air density.
By making use of this symmetry the number of degrees of freedom present in the air domain is nearly halved, while it does not make any difference to the results.

6.4 Result

This chapter presented three methods in order to decrease the number of degrees of freedom of the model. By reducing the size of the air elements, calculating the SPL semi-analytically instead of measuring and making use of the symmetry, a considerable decrease in computational cost of the model is obtained.
Before the mesh refinement study 310.832 degrees of freedom were present in the model for an excitation frequency of 1000 Hz, see Figure 28. After the mesh refinement study only 8.601 degrees of freedom are needed in order to obtain the SPL at a frequency of 1000 Hz, see Figure 29. The maximum SPL difference caused by the model simplifications is 0.7 dB, which is less than the just-noticeable difference of human hearing.

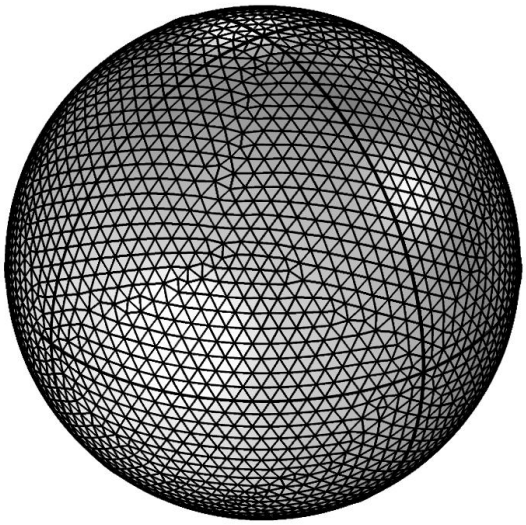

Figure 28: Before the mesh refinement study the model contained maximal 310.832 DOF.

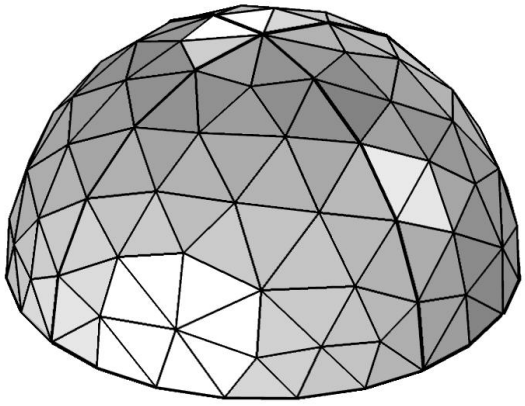

Figure 29: After the mesh refinement study the model contains maximal 8.601 DOF.

7 Mesh refinement study of the wood domain

The previous chapters considered a driven circular plate as a sound source in order to both verify the acoustic part of the model and to perform a mesh refinement study of the air domain.
For the mesh refinement study of the wood domain a geometry is introduced which more resembles the geometry of the final guitar model. A rectangular plate with two added stiffeners, named *braces*, is used for this analysis.

Three configurations of the model are evaluated, using different combinations of solid, shell and beam elements, which are shown in Figure 30. First both the plate and braces are modelled using tetrahedral elements, as shown in Figure 30a. This model is considered to be the most accurate but also the most expensive to solve, as a large number of elements is needed to mesh the plate due to the dimension ratios of a thin-walled structure. For this reason a second configuration is evaluated which meshes the plate with shell elements, see Figure 30b. In a third configuration the number of degrees of freedom is reduced further by modelling the braces with beam elements, which is shown in Figure 30c.

Figure 31 shows the frequency responses of those configurations for five different element sizes. The sizes are indicated qualitatively with the terms 'Extremely coarse', 'Coarser', 'Normal', 'Finer' and 'Extremely fine'. Based on these descriptions the finite element software internally defines the element size properties quantitatively.
It is observed that the model which is meshed with shell and beam elements is able to represent the behaviour of the most expensive model, as shown in Figure 31d. Although some dissimilarities are present, which increase above frequencies of 850 Hz, the response of the model meshed with shell and beam elements is considered to be accurate enough. This enables the user to reduce the number of degrees of freedom significantly.

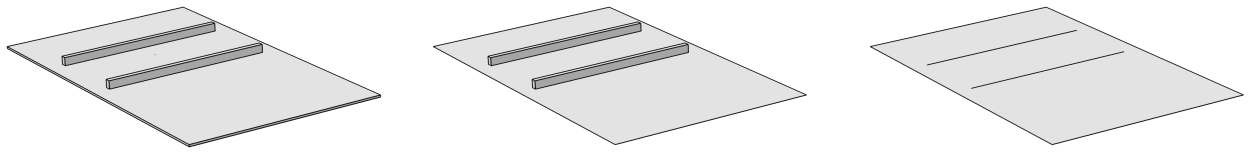

(a) Solid plate, solid bracing (b) Shell plate, solid bracing (c) Shell plate, beam bracing

Figure 30: Modelled geometries of a rectangular plate with two braces.

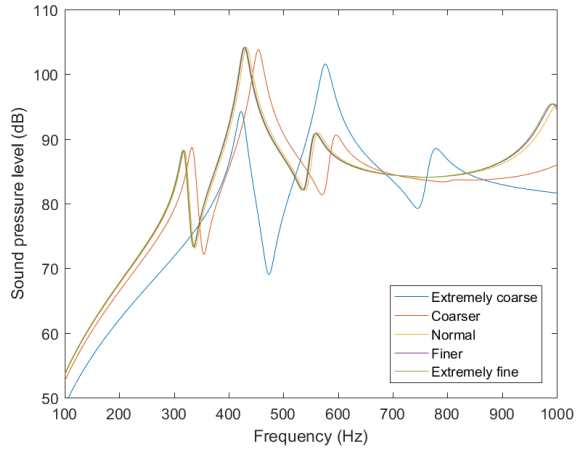

(a) Solid plate, solid bracing

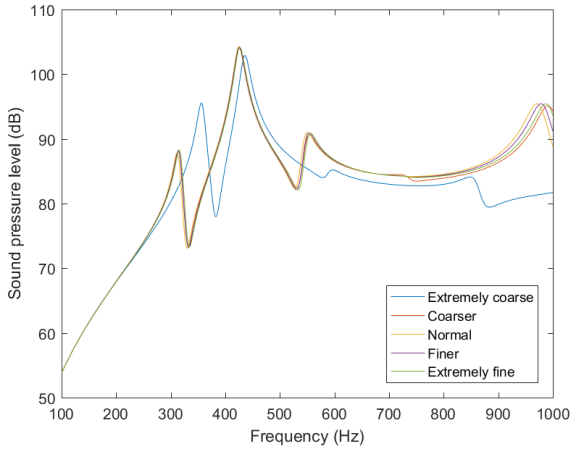

(b) Shell plate, solid bracing

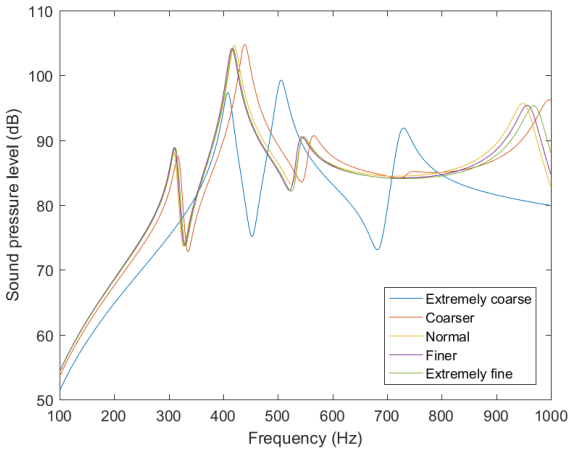

(c) Shell plate, beam bracing

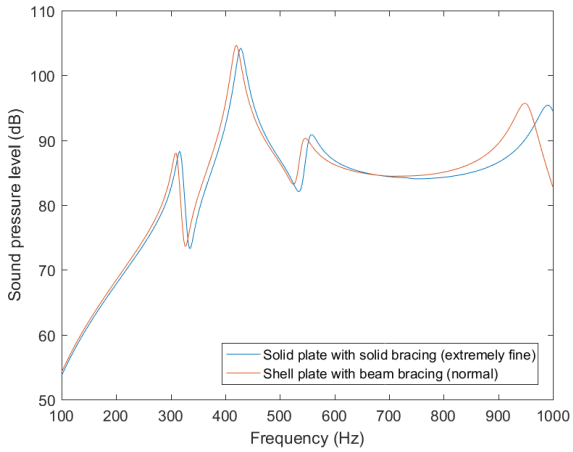

(d) Comparision

Figure 31: Sound pressure levels as obtained by different element types and element sizes.

8 Guitar model

The previous chapters described a method of obtaining the frequency response curve of a driven rectangular wooden structure. In this chapter the geometry of the structure is extended to a geometry which resembles the top plate of an acoustic guitar. There is no need to change anything to the physics involved in the finite element model, as an acoustic guitar its top plate is in fact nothing more than a wooden plate with added stiffeners. The guitar model enables the user to predict the effect of design variable variations on sound pressure levels generated by a guitar. In the next chapter it will be implemented in an optimization algorithm, where it is used to decide which combination of geometric design variables best fits a certain desired frequency response curve.

8.1 Geometry

Figure 32 shows the geometry of the guitar. The red dot denotes the location of the excitation force. The braces of interest for the optimization algorithm are named A, B, C and X. Triangular shell elements are used to mesh the plate, and the braces are meshed with beam elements. The mesh is depicted in Figure 33. This structure contains 9,666 degrees of freedom. Surrounded by the half sphere filled with air the total number of degrees of freedom equals 29,387.

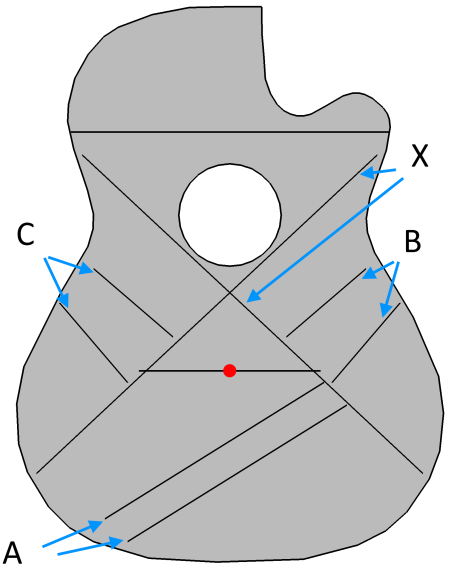

Figure 32: Geometry of the guitar model.

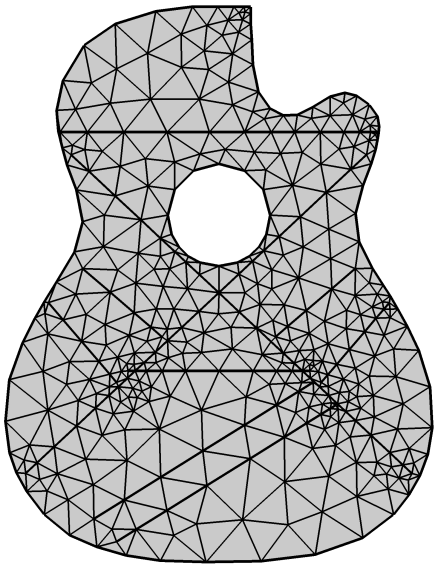

Figure 33: Mesh of the guitar model.

8.2 Simplifications of the model

Some simplifications were made in the model. This sections presents the four simplifications which are considered to be the most important.

Top plate radius

The top plate of a western guitar has a spherical shape, which results in a higher stiffness compared to a flat top plate. Usually the radius is about 12 meters [1]. This radius is not implemented in the guitar model, instead the top plate is flat. Figure 34 shows the response of a spherical top plate as well as the response of a flat top plate. Both plates did not have any braces attached to them. Although in the lower frequency region some differences are observed between the responses, this simplification seems valid. Mind that by attaching the braces the similarity between both responses will be increased, as this decreases the relative difference in stiffness of the structures.

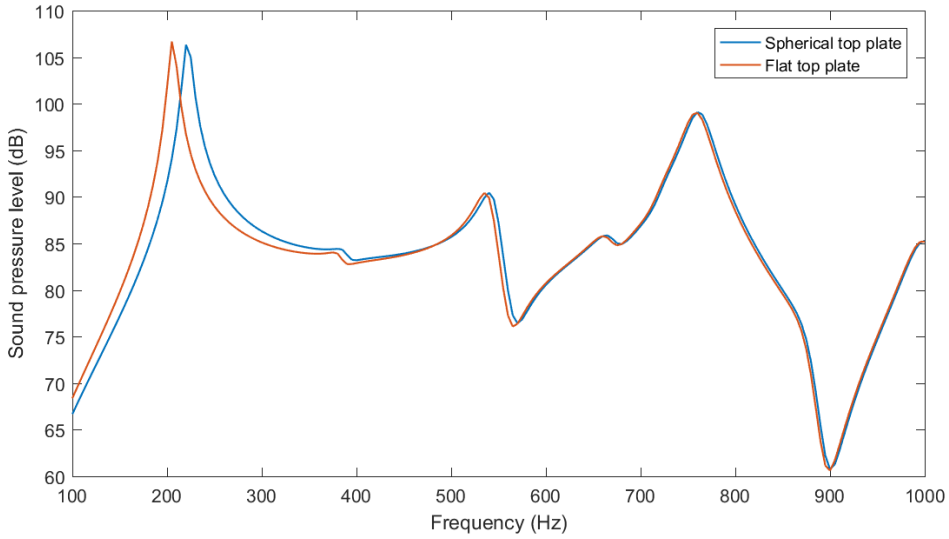

Figure 34: Difference between a spherical and a flat top plate.

Maximum allowable material stres

A tension force of about 750 Newton is applied by the strings on the guitar its top plate. This force acts parallel to the top plate, but due to the distance in between the strings and the top plate it also causes a bending moment. The construction of the guitar has to be able to withstand the stress caused by this force and moment, which could be implemented in the optimization process by introducing a constraint for the maximum allowable material stress. Then for each iteration the algorithm performs an extra operation in order to check the feasibility of the solution. But it was found that the maximum occurring stress does not nearly reach the maximum allowable stress values of wood as found in literature [15]. This is as expected, because a guitar usually does not face instantaneous plastic deformation when the strings are attached or while playing the instrument. Instead, the top plate of an acoustic guitar distorts over time due to creep of the wood [13]. More research is needed in order to find a maximum stress value for which the amount of creep is still just acceptable. For this reason the constraint for the maximum allowable material stress is omitted completely.

Brace profile

As the frequency response properties of a structure mainly depend on the ratio between mass and stiffness, it makes sense to pay attention to the shape of the braces. In general cross sections of braces are convex shaped as non-convex shapes are difficult to obtain with a chisel. Figure 35 shows three different shapes. For all of them the surface area equals 72 mm^2, which means the mass per unit length is also equal. The bottom width of all three braces is 6 mm, ensuring an equal gluing area for all profiles.

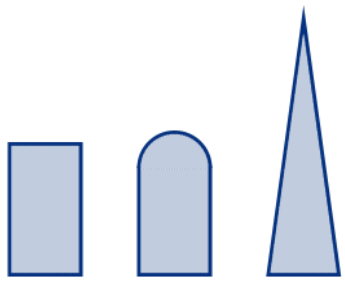

Figure 35: Three brace profiles.

Table 4 lists the area moment of inertia of the three shapes. It shows that a large increase in stiffness is indeed obtained by giving the braces a more complicated shape than just a rectangular one. However, the numerical model only uses rectangular shaped brace profiles. This simplification is justified as the research is aimed at developing a general approach of optimizing the frequency response of a guitar. If the approach would be used to shape the frequency response of a real guitar, one should include more geometric design variables in order to be able to describe and control more complicated brace profiles.

Shape	Area moment of inertia (mm^4)
Rectangular	864
Rectangular, circular top	879
Triangular	2304

Table 4: Area moment of inertia for several cross sections

Anisotropy

Something else which has not been taken into account is the fact that wood is an anisotropic material. The stiffness of wood is different in each of the three principal directions. If one wants to increase the accuracy of the model this anisotropic behaviour should be implemented.

8.3 Verification

The six lowest eigenmodes and eigenfrequencies of the guitar model are showed in Figure 36. Although some simplifications were made in the model, both the shapes of the eigenmodes and the corresponding eigenfrequencies are comparable to the ones found in literature [13].

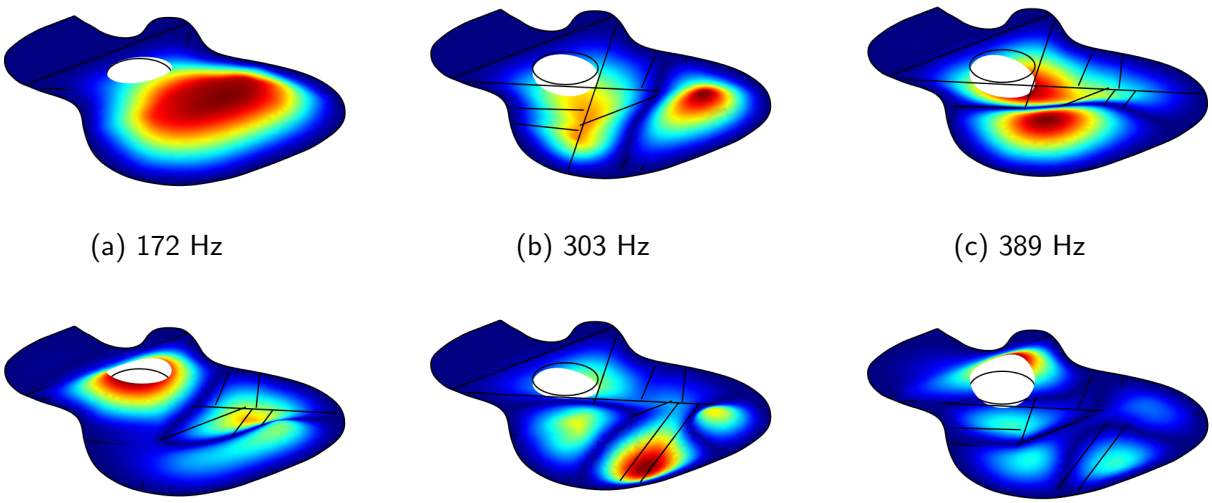

(a) 172 Hz (b) 303 Hz (c) 389 Hz

(d) 510 Hz (e) 582 Hz (f) 752 Hz

Figure 36: Six lowest eigenmodes of the guitar model.

Part III
Application of the model

9 Dynamic response optimization

The optimization algorithm calculates an optimal combination of geometric design parameters in order for the structure to approximate a certain desired frequency response. This chapter first presents the mathematical problem statement of the optimization problem. Next, an optimization is performed which involves only two design variables. The response of two different optimization algorithms is compared, and based on the results an algorithm is chosen which is used for the full problem, which involves six design variables. The flexibility of adjusting the frequency response of a structure depends on the number of design variables used. It is chosen to use six variables in order to describe the geometry as this seems an acceptable compromise between flexibility and computational cost. Finally an example is presented which corrects for the differences that occurred in the frequency response caused by material property variations. Because the optimization algorithm can probably not correct for variations in material damping, this property remains unchanged in all examples.

9.1 Mathematical problem statement

Mathematically the operation is performed by minimizing an objective function $f(\mathbf{x})$ [39]. Each of the design variables is subjected to both a lower and an upper bound. The design variables are contained by vector $\mathbf{x}$, and their lower and upper bounds by vectors $\underline{\mathbf{x}}$ and $\overline{\mathbf{x}}$. This results in a mathematical problem statement which is defined as

$$\begin{aligned} &\min_{\mathbf{x}} f(\mathbf{x}) \\ \text{subject to:} \quad &\underline{\mathbf{x}} \leq \mathbf{x} \leq \overline{\mathbf{x}} \end{aligned} \tag{16}$$

The objective is defined as the squared difference of the vectors containing current and desired sound pressure levels at chosen frequency intervals. Mathematically the objective function is described as

$$f(\mathbf{x}) = \|\mathbf{y}_t - \mathbf{y}(\mathbf{x})\|_2^2 \ , \tag{17}$$

where the desired SPL is defined by vector $\mathbf{y}_t$. The current SPL is a function of the design variables $\mathbf{x}$ and is denoted by $\mathbf{y}(\mathbf{x})$.

The size of the vectors containing the sound pressure levels depends on the frequency interval chosen by the user. A smaller interval will result in a more detailed frequency response curve, but also more evaluations of the finite element model are needed. It was found that with a frequency interval of 10 Hz detailed curves are obtained while the computational effort still is acceptable. All models in this research are evaluated for a frequency range of 900 Hz, which means 91 evaluations of the finite element model are needed for each function evaluation of the optimization algorithm. Mind that because of this the evaluations of the finite element model are easily parallelized, regardless of the type of optimizer used.

One or more stopping conditions for the optimization algorithm have to be defined. More research is needed to find out to what extent the frequency response curve of a guitar top plate should match the desired curve in order for the final instrument to sound exactly the same. During the literature study it was found that the just-noticeable difference for human hearing lies between 1 and 3 dB. Based on this it is assumed that if throughout the whole frequency range the difference between the current and desired SPL is smaller than 1 dB, it is probably impossible for the listener to distinguish

between the desired response and the optimum found by the algorithm. The first stopping condition of the algorithm is based on this.
Unfortunately it is not guaranteed that the optimization algorithm is able to satisfy the first stopping condition. For this reason a second stopping condition is defined, which stops the optimization if during three successive iterations the objective value decreases less than ten percent.

9.2 Optimization of the frequency response curve

Figure 37 shows an arbitrary desired response (blue) and the response from an arbitrary initial design (red). Both responses are a result of the same model, but different values for the design variables are used. In this example the design variables are the height of the X-braces and the thickness of the guitar's top plate, see Figure 38. To make the objective more visual vertical lines are drawn in the figure. The objective value equals the sum of the squared lengths of the green lines, and it is the optimization algorithm its task to minimize this sum. As in this example the desired response is generated with the same model as the one used to calculate the objective value, by the end of the optimization process the algorithm should have found a combination of design variables for which the objective value equals zero.

First a nonlinear least squares optimizer is used, which uses a trust region algorithm. Starting from the chosen initial variable values it needs 12 iterations to approximate the optimum value, as illustrated in Figure 39. Since the finite element model does not provide gradient information, for each iteration the gradients are obtained by a finite difference method. This brings the total number of function evaluations to 36.

The same optimization problem is also solved with a Nelder-Mead algorithm, of which the progress is shown in Figure 40. The surface is semi-transparent as otherwise the triangles located below the surface area would become invisible. This algorithm needs 52 function evaluations, which is more than the trust region algorithm. Another drawback of the Nelder-Mead algorithm is that when the number of design variables is increased its performance compared to a trust region algorithm probably decreases [39]. As the full problem contains six design variables it is decided that from now on the trust region algorithm will be used instead of a Nelder-Mead algorithm.

Because this example uses only two variables it is possible to generate the depicted surface plots. Mind that such plots are obtained by evaluating so many design variations that a three-dimensional view of the objective value for a range of input variables can be made. Once the complexity of the optimization problem increases this is not possible anymore in a reasonable amount of time. One has to rely on the optimum found by the algorithm, without being able to check it in a surface plot of the objective value.

This first example showed that satisfactory results can be obtained by applying the approach as presented in the previous section. The next two subsections contain more challenging optimization problems in order to show the possibilities of the optimization algorithm. Mind that more approaches of defining an objective function and applying an optimization algorithm are available. One of them is presented in A.5.

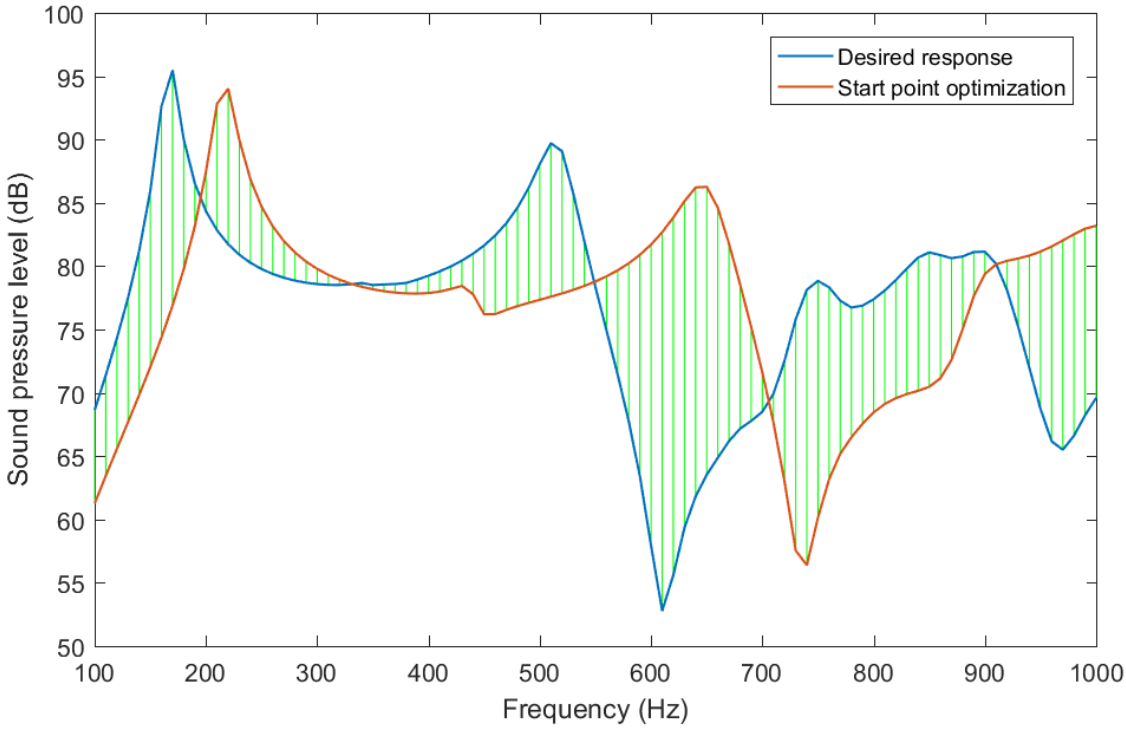

Figure 37: Desired (blue) and initial (red) response. The objective is defined as the sum of the squared lengths of the green lines.

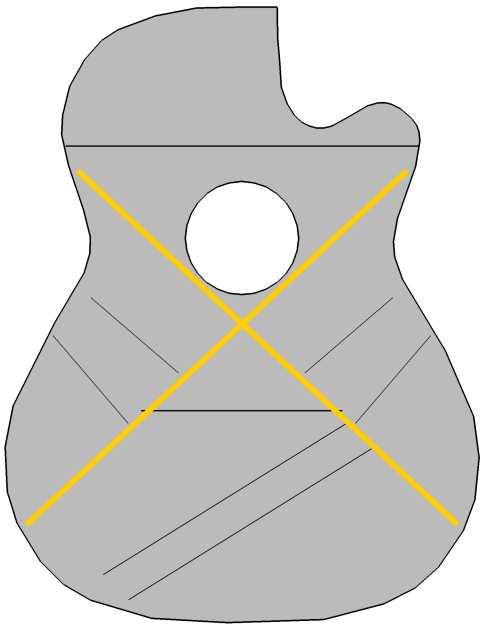

Figure 38: The thickness of the plate and the height of the X-braces (yellow) are design variables in this example.

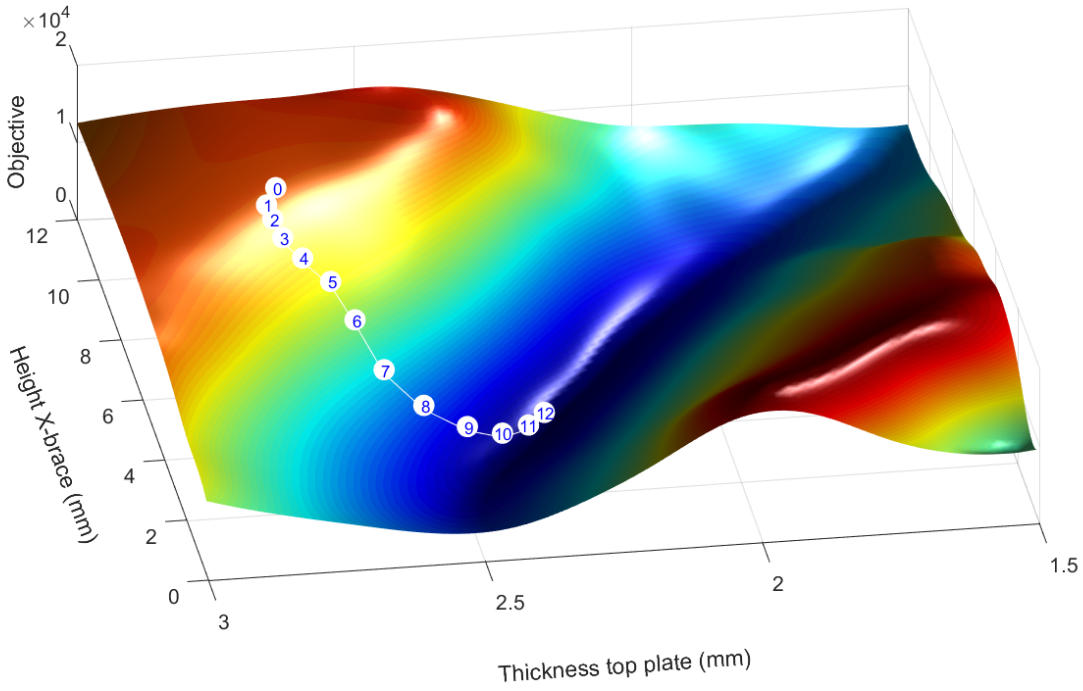

Figure 39: Iterations of the optimization if a trust region algorithm is used.

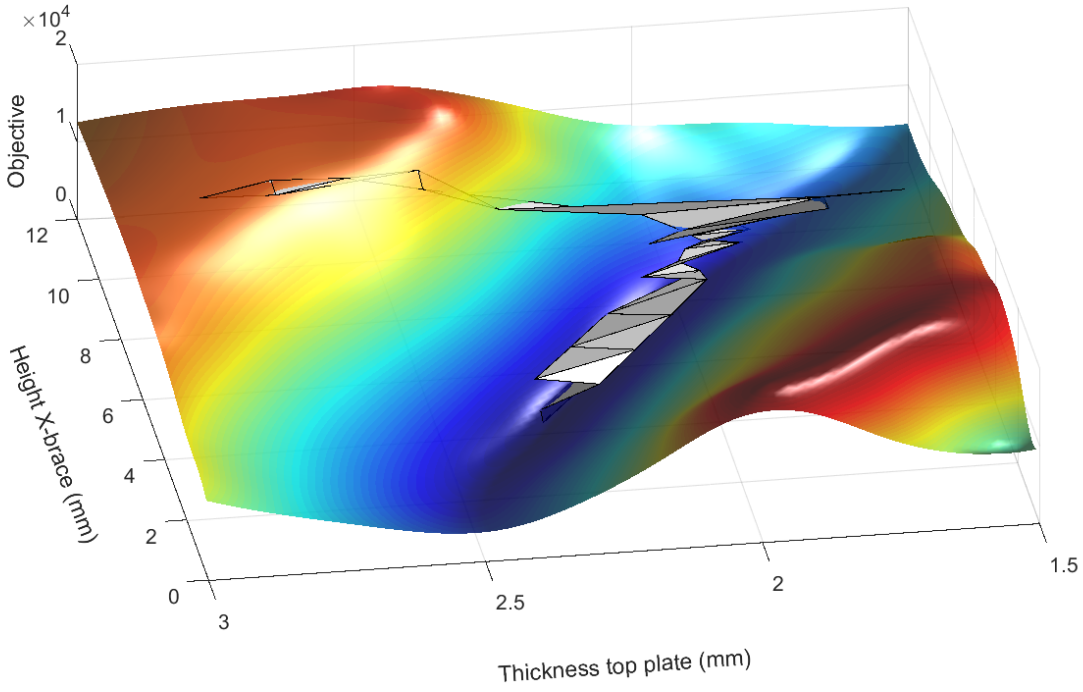

Figure 40: Iterations of the optimization if a Nelder-Mead algorithm is used.

Optimization of six design variables

Instead of only the thickness of the plate and the height of the X-braces as design variables, more design variables are introduced. In the example in this section also the width of the X-braces and the heights of the yellow, green and purple bracing pairs in Figure 41 are design variables. The height of both braces of a pair is equal. Again the desired response is generated with the same model as the one used to calculate the objective value.

Figure 42 shows the result of an arbitrary optimization of those six variables. The evolution of the design variables and objective value during the optimization process is illustrated in Figure 43. The colors of the lines match the colors of the braces as indicated in the aforementioned Figure 41.
It is observed that in 10 iterations an accurate fit of the desired response is reached. The optimization stopped because after those 10 iterations the difference between the current and desired response was smaller than 1 dB throughout the whole frequency range.

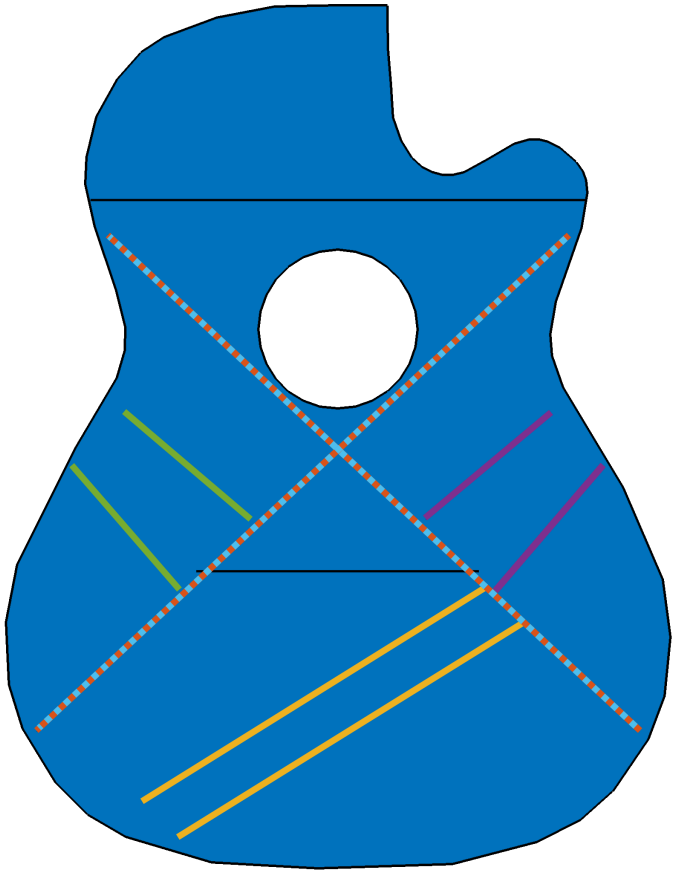

Figure 41: In this example the design variables are the thickness of the plate, the height of the yellow, purple and green braces and both height and width of the red-blue dotted brace.

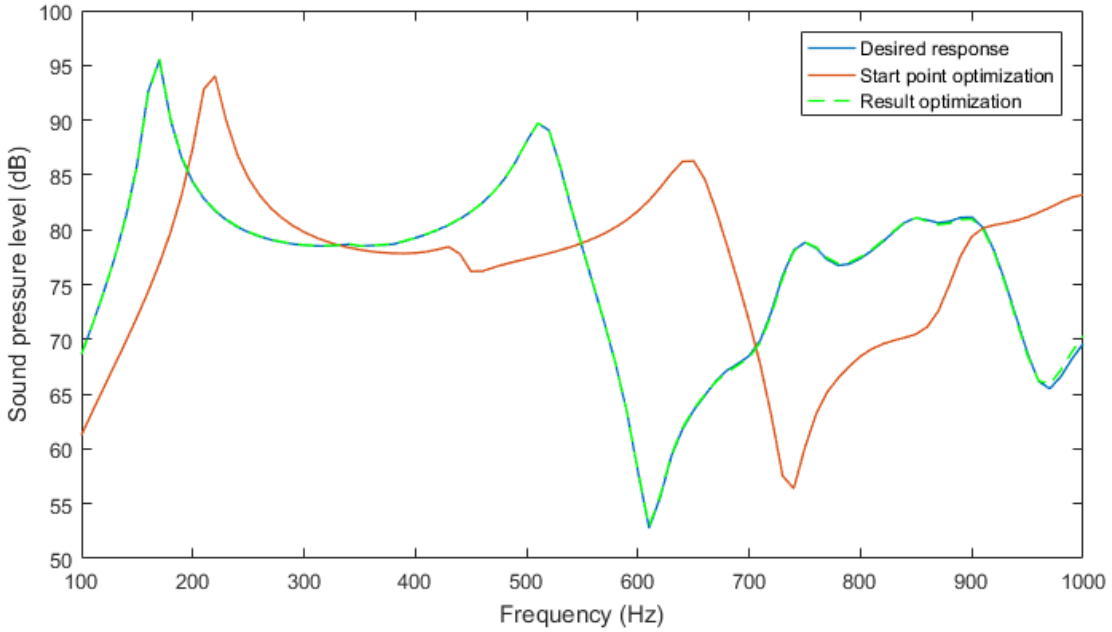

Figure 42: Desired response, initial response and the optimization result.

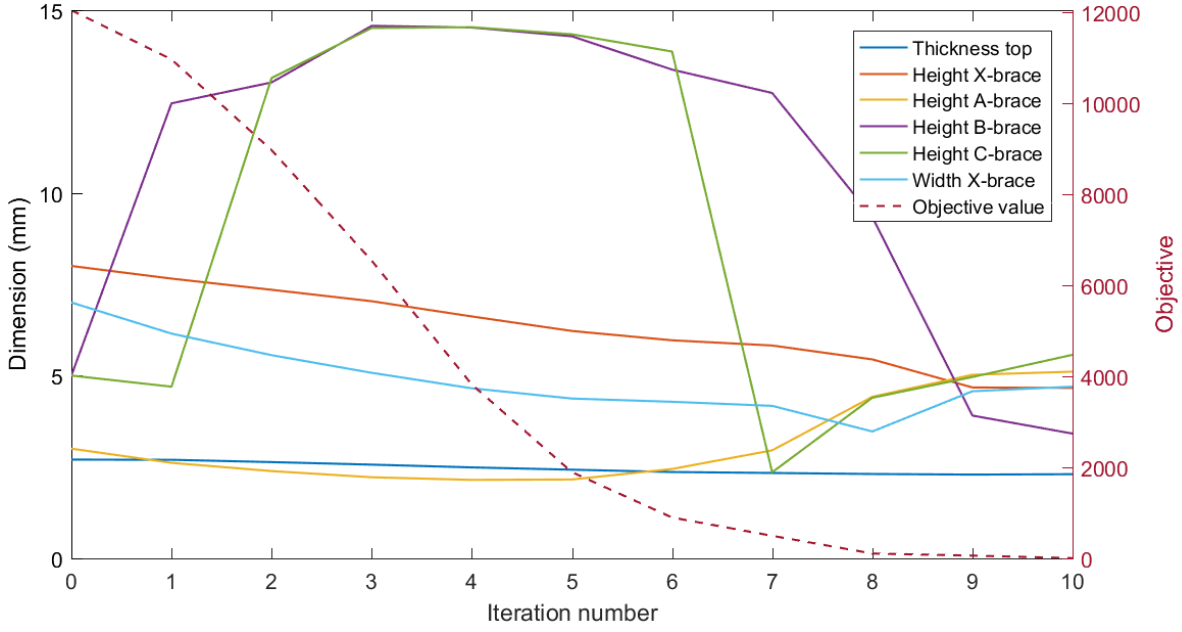

Figure 43: Evolution of design variables and objective during optimization process.

Optimization with different material properties

In this final example the material properties of the model used to approximate the desired response are different from the material properties as applied in the model which generated this desired response. The goal of the optimization algorithm is to correct for the SPL differences caused by the material property variations. The design variable values of the initial response and the desired response are equal.

The quality of the wood used for the top plate is considered to be much more important than the wood quality of the braces [3]. For this reason we will only change the material properties of the top plate. The density of the top plate is increased with 10%, and its Young's modulus is decreased with 10%. Both the isotropic structural loss factor and the Poisson's ratio are unchanged.
The chosen percentage for the increase of the density equals about five standard deviations of high quality top plate wood [16]. The chosen percentage for the stiffness decrease equals about two and a half times the standard deviation.

Figure 44 shows the initial and the desired response, as well as the result of the optimization. Between 200 and 500 Hz the final response is slightly different from the desired response, but in general they are very similar. It can be concluded that the optimization algorithm is capable of correcting the SPL caused by material property variations.
Figure 45 shows the evolution of the design variables and the objective value during the optimization process. It is seen that in each of the first five iterations the objective value drops considerably. As during the last three iterations the decrease of the objective value was less than ten percent, the optimization stopped due to the second stopping condition. Table 5 lists the values of the design variables of both the initial and the final design.

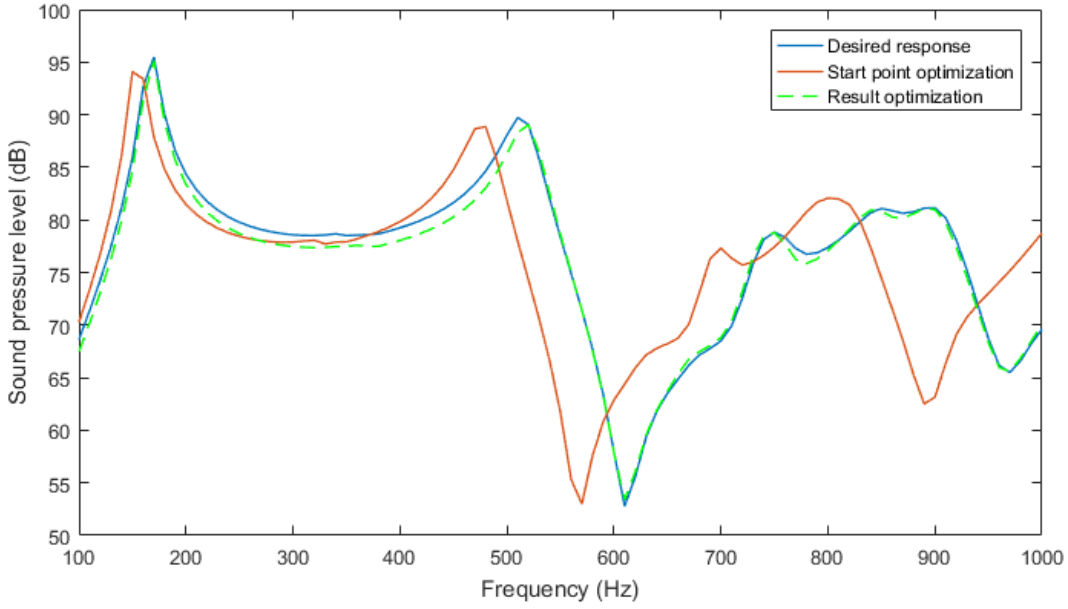

Figure 44: Desired response, initial response and the optimization result.

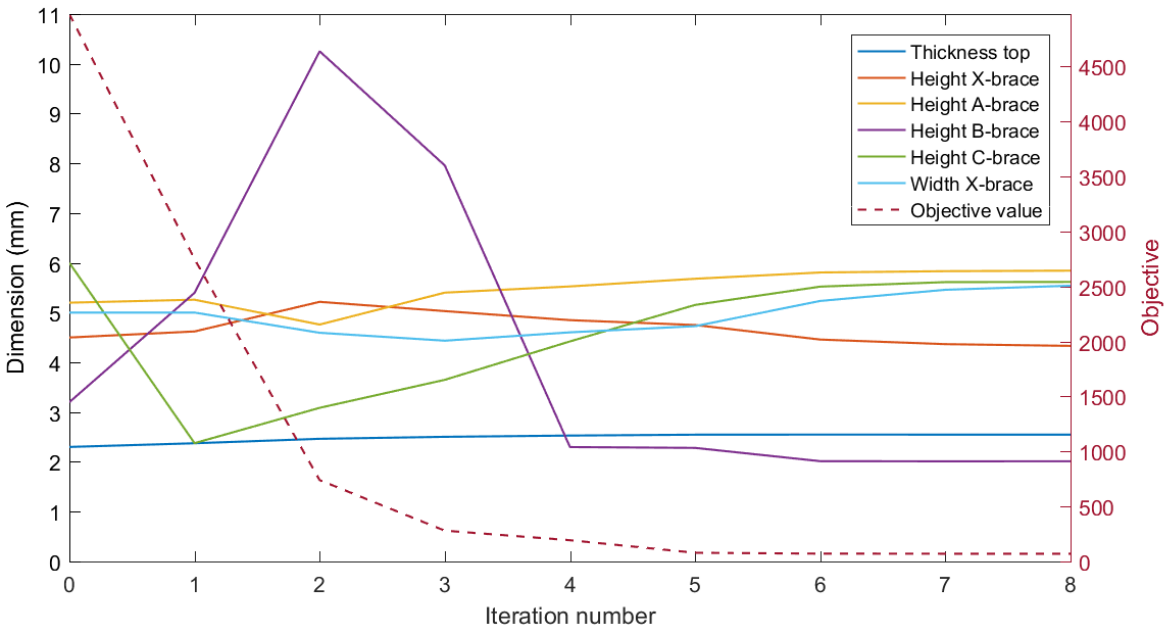

Figure 45: Evolution of design variables and objective during optimization process.

	Initial dimension (mm)	Final dimension (mm)
Thickness top	2.30	2.55
Height X-brace	4.50	4.33
Height A-brace	5.20	5.84
Height B-brace	3.20	2.01
Height C-brace	6.00	5.62
Width X-brace	5.00	5.54

Table 5: Initial and final design variable values.

10 Conclusion

The goal of this research was to find a method which is both able to improve the consistency between mass-produced instruments and to decrease the required building time of handbuilt guitars. In order to achieve a satisfactory result it was investigated if the perceived sound produced by a guitar is controllable by using dynamic response optimization methods in order to adjust geometric design parameters during the production process. Based on the results of the optimization algorithm it is concluded that it is indeed possible to control the perceived sound produced by a guitar, by applying this method.

The approach presented in this research can be implemented in an industrial production process, which enables one to decrease the differences between instruments which are supposed to sound the same. If it is a drawback that by using the current optimization algorithm guitars may take up more time on the assembly line than desired, the possibilities of parallel computing should be explored. As many function evaluations are needed for each combination of design variables, the algorithm is easily parallelized.
In a similar way traditional luthiers can also benefit from the method described in this study. Maybe the most difficult task of a luthier is to find a guitar which sounds special to him or her. The optimization algorithm is not able to help with this. But once one has found a response which turns out to produce a desirable instrument, it can be reproduced much faster.

Some aspects need to be worked out further before the approach presented in this research can be implemented in a production process. For example, we did not consider variations in the material damping as the optimization algorithm probably cannot correct for them. Because of this it will be necessary to preselect woods based on their damping coefficient, in order to maximize the consistency of the production process. Another point of attention is that it is yet unknown to what extent the response curve of an instrument should match the desired curve in order to sound exactly the same. However, the theoretical background will definitely be useful in order to improve consistency between instruments by using frequency response measurements during the building process. The next chapter presents some additional recommendations for further research.

11 Further research

11.1 Extracting material properties

Material properties such as the wood's density, damping coefficient and modulus of elasticity have to be known in order to simulate its dynamic behaviour in the finite element model. As explained in the introduction of this report the properties of wood vary from tree to tree. Measuring those properties for each used piece of wood manually would be a labour intensive process.
This step can be bypassed by starting each build from a basic design with known dimensions. The optimization model could be adjusted so that the information obtained by an initial frequency response measurement is used to extract the material properties of the various used pieces of wood.

11.2 Refinement of the oscillator model

The oscillator model uses only one driving point and, unlike the strings, the driving force acts perpendicular to the top plate. Probably the frequency response of a guitar is better characterized by using several frequency response curves instead of just one, each having a different driving point. Figure 46 proposes three measurement locations and directions.
Also, it should be investigated if the effect of coupling between strings and the guitar body leads to noticeable inaccuracies in the modelled sound pressure level.
With those improvements the model might be suitable for performing reliable transient simulations. Instead of just looking at the difference between two curves in order to examine the effect of design variations, it would be very interesting to be able to actually hear the difference by simulated sounds.

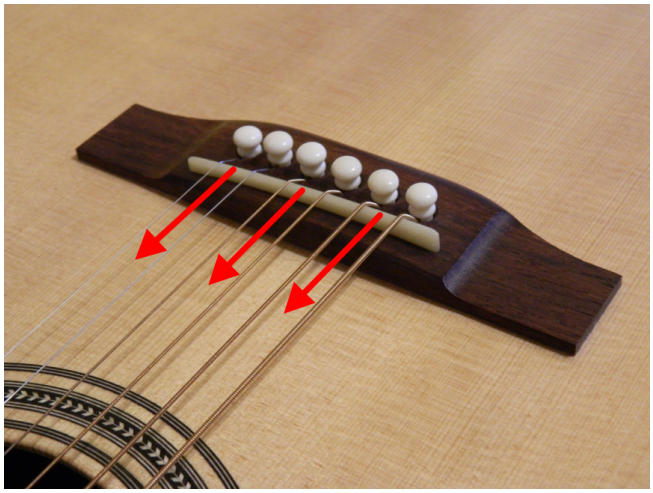

Figure 46: Different driving point.

11.3 Dynamic substructuring

The optimization procedures used in this study always evaluate the system as a whole during solving. By applying dynamic substructuring techniques the instrument can be divided into subparts. The system matrices are reorganised such that the degrees of freedom belonging to the same subpart are grouped. The advantage of this method is that for iterations of design variables which do not affect all subparts, it is not necessary to solve the complete system of equations. Only the parts of the

system matrices belonging to the modified subparts have to be evaluated again, which will decrease computational costs [40].

11.4 Refinement of the bracing pattern

The bracing pattern used in the interior is probably not the most efficient geometry in order to control the individual eigenmodes. In fact, the usual locations of the braces have not really changed since the first literature about plate dynamics appeared in 1877 (The Theory of Sound, by Lord Rayleigh). Possibly this refinement can be achieved with topology optimization.

Guitar builders usually try to remove as much mass as possible, as this makes the guitar more responsive [3]. But if one just wants to fit the frequency response curve of a build in progress to a target curve, removing mass of the braces might not be the most efficient approach. A lightweight bracing design which ensures the structure being able to withstand the string force, in combination with point masses to control the relative response of the eigenmodes may result in a faster building process.

11.5 Guitar 2.0

The exploratory research described in this report on modelling and optimizing the response of acoustic guitars, together with the above suggestions for further research, opens up an incredible amount of new possibilities for the way guitars are designed and built. These developments might even be necessary as high quality woods are getting scarce.
Instead of building the guitar's soundboard out of a wooden plate with braces glued to it, an interesting approach would be to mill it from a thicker, synthetic plate. During the production process measurements can be taken in order to shape the frequency response to a desired target.
Another possibility is 3D printing, although it might be difficult to find a material which is both 3D printable and capable of producing a certain desired frequency response.

References

[1] William R. Cumpiano, Jonathan Natelson, *Guitarmaking: Tradition & Technology*, Chronicle Books, San Francisco, 1987.

[2] John S. Bogdanovich, *Classical Guitar Making: A Modern Approach to Traditional Design*, Sterling, New York, 2007.

[3] Ervin Somogyi, *The Responsive Guitar*, Luthiers Press, 2011.

[4] Ian M. Firth, *Physics of the guitar at the Helmholtz and first top-plate resonances*, School of Physical Sciences, University of St. Andrews, Fife, Scotland, 1976.

[5] Ove Christensen, Bo B. Vistisen, *Simple model for low-frequency guitar function*, Journal of the Acoustic Society of America, Vol. 68, 1980.

[6] Ove Christensen, *Quantitative models for low frequency guitar function*, Journal of Guitar Acoustics, Vol. 6, 1982.

[7] Ove Christensen, *An Oscillator Model for Analysis of Guitar Sound Pressure Response*, Medical Physiology Department A, The Panum Institute, University of Copenhagen, 1984.

[8] John E. Popp, *Four mass coupled oscillator guitar model*, Journal of the Acoustic Society of America, Vol. 131, 2012.

[9] B. Richardson et al, *The three-mass model for the classical guitar revisited*, Société Française d'Acoustique, Acoustics 2012, Nantes, France, 2012.

[10] Richard Mark French, *Structural modification of stringed instruments*, Mechanical Systems and Signal Processing, Vol. 21, 2007.

[11] D. P. Hess, *Frequency response evaluation of acoustic guitar modifications*, Savart Journal, 2013.

[12] Howard Wright, *The acoustics and psychoacoustics of the guitar*, Department of Physics and Astronomy, University of Wales, College of Cardiff, 1996.

[13] Richard Mark French, *Engineering the guitar*, Springer, West Lafayette, Indiana, 2009.

[14] Hill, B.E. Richardson, S.J. Richardson *Acoustical parameters for the characterisation of the classical guitar*, Acta Acustica united with Acustica Vol. 90, 2004.

[15] Voichita Bocur, *Acoustics of wood*, Second edition, Springer, Berlin, 2006.

[16] Max Roest, *Design of a composite guitar*, Master thesis, TU Delft, Delft, 2016.

[17] Elejabarrieta, Ezcurra, Santamaria, *Evolution of the vibrational behaviour of a guitar soundboard along successive construction phases by means of the modal analysis technique*, The Journal of the Acoustical Society of America, Vol. 108, 2000

[18] Elejabarrieta, Santamaria, *Air cavity modes in the resonance box of the guitar: The effect of the soundhole*, Journal of Sound and Vibration, Vol. 252, 2001.

[19] Elejabarrieta, Ezcurra, Santamaria, *Coupled modes of the resonance box of the guitar*, The Journal of the Acoustical Society of America, Vol. 111, 2002

[20] Ezcurra, Elejabarrieta, Santamaria, *Fluid-structure coupling in the guitar box: numerical and experimental comparative study*, Applied Acoustics, Vol. 66, 2005.

[21] Jürgen Meyer, *Quality aspects of the guitar tone*, Royal Swedish Academy of Music No. 38, 1983.

[22] Boullosa, Orduna-Bustamante, Perez Lopez, *Tuning characteristics, radiation efficiency and subjective quality of a set of classical guitars*, Applied Acoustics, Vol. 56, 1999.

[23] Torres, Jess A.; de Icaza-Herrera, Miguel; Castao, Vctor M. *Guitar Acoustics Quality: Shift by Humidity Variations*, Acta Acustica united with Acustica, Volume 100, May/June 2014.

[24] Stereokroma TV, *Making a Handmade Guitar - Où se trouve: Greenfield Guitars*, Documentary, 2016.

[25] S. Šali, J. Kopač, *Measuring a frequency response of a guitar*, IMAC XVIII, 2000.

[26] Thomas D. Rossing, *The Science of String Instruments*, Springer, New York, 2010.

[27] P.J.M. Roozen-Kroon, *Structural optimization of bells*, TU Eindhoven, Eindhoven, 1992.

[28] Nobuyuki Okubo et al, *Vibration and Acoustic Analysis of Acoustic Guitar in Consideration of Transient Sound*, Rotating Machinery, Hybrid Test Methods, Vibro-Acoustics & Laser Vibrometry, Volume 8, Springer, 2016.

[29] Gyung-Jin Park, *Analytic Methods for Design Practice*, Springer, London, 2007.

[30] Franklin et al, *Feedback Control of Dynamic Systems*, Sixth edition, Pearson, 2010.

[31] Cremer, Heckl, Petersson, *Structure-Borne Sound*, Third edition, Springer, Berlin, 2005.

[32] Rao, *Mechanical Vibrations*, Fourth edition, Prentice Hall, Singapore, 2005.

[33] R. Munnig Schmidt et al, *The Design of High Performance Mechatronics*, Second edition, Delft University Press, Amsterdam, 2014.

[34] Robert D. Cook et al, *Concepts and applications of finite element analysis*, Fourth edition, Wiley, New York, 1974.

[35] COMSOL, *Acoustics Module User's guide*, COMSOL Multiphysics version 5.2.

[36] Warren C. Young, Richard G. Budynas, *Roarks Formulas for Stress and Strain*, Seventh edition, McGraw-Hill, New York, 2002.

[37] Michel Géradin, Daniel J. Rixen, *Mechanical vibrations*, Third edition, Wiley, Chichester, 2015.

[38] Frank M. White, *Fluid Mechanics*, Sixth edition, McGraw-Hill, New York, 2009.

[39] Panos Y. Papalambros, Douglass J. Wilde, *Principles of Optimal Design*, Second edition, Cambridge University Press, Cambridge, 2000.

[40] D. de Klerk, D. J. Rixen, S. N. Voormeeren, *A General Framework for Dynamic Substructuring: History, Review and Classification of Techniques*, AIAA Journal, 46(5), 2008.

[41] Daniel J. Rixen, *Mechanical Analysis for Engineering*, Lecture notes TU Delft course WB1450-05, 2011.

[42] Sanjeev R. Kulkarni, *Lecture Notes Electrical Signals and Systems*, Princeton University course, 2001.

[43] S. Errede, *The Human Ear - Hearing, Sound Intensity and Loudness Levels*, Department of Physics, University of Illinois, Illinois, 2016.

A Appendix

A.1 Software

The software packages used in this research are COMSOL Multiphysics 5.2 and MATLAB R2016a. Several add-on modules are used in COMSOL; the Structural Mechanics Module, the Acoustics Module and the LiveLink for MATLAB. The models which are described in this report are not built in COMSOL itself; instead they are programmed via MATLAB. The two software programs are able to communicate via the LiveLink for MATLAB. Although most of the models presented in this report can be build and solved while solely using COMSOL, involving MATLAB gives the user many more possibilities in terms of efficiently building and solving the model successively from within loops in order to control parameter values.

A.2 Acoustic boundary conditions

Spherical wave radiation:

$$-n \cdot \left(-\frac{1}{\rho_{\mathrm{c}}}(\nabla p_{\mathrm{t}} - q_{\mathrm{d}})\right) + \left(ik_{\mathrm{eq}} + \frac{1}{r}\right)\frac{p}{\rho_{\mathrm{c}}} - \frac{r\Delta_{\mathrm{T}}p}{2\rho_{\mathrm{c}}(1 + ik_{\mathrm{eq}}r)} = Q_{\mathrm{i}}$$

Interior sound hard boundary:

$$-n \cdot \left(-\frac{1}{\rho_{\mathrm{c}}}(\nabla p_{\mathrm{t}} - q_{\mathrm{d}})\right) = 0$$

Acoustic-Structure boundary:

$$-n \cdot \left(-\frac{1}{\rho_{\mathrm{c}}}(\nabla p_{\mathrm{t}} - q_{\mathrm{d}})\right) = n \cdot u_{\mathrm{tt}}$$

A.3 Verification finite element model

Deflection of a clamped circular plate
A force *W* acting in the middle of a flat circular plate of constant thickness with radius *a* causes a maximum displacement of [36]:

$$y_{\max} = \frac{-Wa^2}{16\pi D}$$

D is the flexural rigidity:

$$D = \frac{Et^3}{12(1 - v^2)}$$

In this equation is *E* the Young's modulus of elasticity, *t* the plate thickness and *v* the Poisson's ratio.

When the equations above are used with the values as listed in the table, a displacement of 0.03502 millimeters is obtained. The maximum displacement of the finite element model excited at 1 Hz is 0.03569 millimeters. This is a 2% difference.

Eigenfrequencies of a clamped circular plate
In the equation below, *a* refers to the mass per square meter. For the first, second/third and sixt eigenmode of a clamped circular plate values for α are 1.015, 1.468 and 2.007.

$$\omega_{0,i} = \alpha_i^2 \frac{\pi^2}{a^2} \sqrt{\frac{D}{m}}$$

A.4 Mesh refinement study data

The ordering of the table's rows is equal to the legends of the corresponding figures. Mean difference, standard deviation and maximal difference are calculated with respect to the result which is considered to be the most accurate. All values are in decibel.

Mean difference	Standard deviation	Maximal difference
0.83603	1.1598	5.489
0.23144	0.26955	1.541
0.05794	0.07494	0.42651
0.016939	0.033117	0.19503
0	0	0

Table 6: Belongs to Figure 22

Mean difference	Standard deviation	Maximal difference
0.83603	1.1598	5.489
0.048008	0.25322	0.69225

Table 7: Belongs to Figure 26

Mean difference	Standard deviation	Maximal difference
-3.7486	6.599	12.943
-1.3995	4.2998	15.241
-0.19312	0.85979	3.0845
-0.042259	0.24251	0.87838
0	0	0

Table 8: Belongs to Figure 31a

Mean difference	Standard deviation	Maximal difference
-1.7079	4.9599	15.099
-0.080562	0.44539	1.3957
0.16962	1.0884	3.7858
0.10277	0.51086	1.8388
0	0	0

Table 9: Belongs to Figure 31b

Mean difference	Standard deviation	Maximal difference
-3.5103	6.186	14.719
-0.048876	2.9041	9.2665
0.22183	1.4243	3.3748
0.08132	0.84707	2.2971
0	0	0

Table 10: Belongs to Figure 31c

Mean difference	Standard deviation	Maximal difference
0.5188	2.606	6.1562

Table 11: Belongs to Figure 31d

A.5 Indirect optimization of frequency response curve

As in the frequency response curves the damping properties of a guitar are only captured by the sharpness of the peaks, one might want to emphasize those frequency regions by involving the Q-values of the peaks in the objective function.

Another possibility instead of direct optimization of the frequency response curve to a desired one, is to first characterize the response of a design by its fitted oscillator model parameter values. The objective function would be the mean squared error of vectors containing parameter values of both the current and desired response. As explained in Chapter 4, the parameters of this model represent the eigenfrequency, equivalent surface area, effective mass and Q-value. Because of the different meanings and dimensions they should appear scaled and weighted in the objective function.
This approach will result in a nested optimization procedure since for each iteration of the geometric design variables the oscillator model parameters have to be extracted. If gradients of the oscillator parameter values are calculated, their value will depend on the quality of the curve fit. Because of this the curve fitting algorithm has to be very robust; it should be able to perform hundreds of consecutive curve fits without getting stuck in a local optimum.
Also care must be taken as during the optimization process unusual combinations of design variables are encountered. It is not guaranteed that the frequency response of such a combination is accurately captured by the oscillator model, because higher eigenmodes might enter the frequency range of interest.

It was found that by applying this indirect approach it was difficult to obtain satisfying results. Apart from that it is not known to what extend it is possible to control the damping of the structure, which might decrease the need of representing damping in an objective function.